Project Report
on

Design and Optimization of Shuriken Shaped Nanorectenna for Infrared Detection and Harvesting

A thesis submitted in partial fulfillment of the requirements for the award of the degree of

Master of Technology
in
Microwave and Optical Communication Engineering

Submitted by
Shubhanshi Sharma
2K15/MOC/18

Under the guidance of
Dr. Yogita Kalra
Assistant Professor
Department of Applied Physics

Department of Electronics and Communication
and
Department of Applied Physics
Delhi Technological University
Delhi, India – 110042

June 2017

Certificates

Department of Electronics and Communication
and
Department of Applied Physics

Delhi Technological University

This is to certify that the dissertation entitled **DESIGN AND OPTIMIZATION OF SHURKIEN SHAPED NANORECTENNA FOR INFRARED DETECTION AND HARVESTING** is a bonafide record presented by Shubhanshi Sharma during IVth Semester, June 2017 in partial fulfilment of the requirements of the degree of Master of Technology in Microwave and Optical Communication Engineering under my supervision and guidance.

Dr. Yogita Kalra
Assistant Professor
Project Guide

Dr. S.Indu
Professor
Head Of Department,ECE

Declaration

I hereby declare they all the information in this document has been obtained and presented in accordance with academic rules and ethical conduct. This report is my own, unaided work. I have fully cited and referenced all material and results that are not original to this work. It is being submitted for the degree of Master of Technology in Engineering at Delhi Technological University. It has not been submitted before for any degree or examination in any other university.

Shubhanshi Sharma
2K15/MOC/18
M.Tech MOCE

Abstract

In this project nanorectenna has been studied and optimized for energy harvesting. Nanorectenna is a device which consists of nanoantenna and a MIM diode, which rectifies the Alternating current into Direct current. To begin with, the optoelectronic properties of the noble metals as gold and copper have been studied, which show that at Terahertz frequency metals have complex dielectric constants and behave as dielectric. Furthermore, Shuriken shaped plasmonic nanoantenna has been designed and optimized to test its near field enhancement capabilities for implementation in infrared detection. Near field resonant properties and far field characteristics of a single Shuriken type as well as coupled Shuriken type nanoantenna have been numerically investigated. On account of simple geometry, the proposed structure is not supposed to pose any difficulty during fabrication. In addition, here the use of nanoarray instead of single elements has been investigated. The aim is to increase the overall captured electric field. To benefit from this enhancement, the rectifier is realized between the overlapped antennas arms using an insulator. The thin film of CuO has been used as metal/insulator/metal(MIM) diode which offers low zero bias resistance, thus improving the impedance matching with the antenna. The result shows that performance of shuriken shaped nanoantenna is much better than bow tie nanoantenna in terms of electric field enhancement and polarization.

Acknowledgements

I would like to express my sincere gratitude to my project supervisor, Dr. Yogita Kalra, for her supervision, invaluable guidance, motivation and support throughout the extent of the project. I have benefited immensely from her wealth of knowledge.

I would like to thank Phd Scholar Mr. Nishant Shankhwar for his precious suggestions, technical and moral support during the course of this project.

My gratitude is extended to my colleagues and friends who have not been mentioned here personally in making this project a success.

Last but not the least, I want to thank my parents, for inculcating good ethos, as a result of which I am able to do my post-graduation from such an esteemed institution. I would thank my friends for believing in my abilities and for always showering their invaluable support and constant encouragement.

Shubhanshi Sharma
2K15/MOC/18
M.Tech MOCE

Contents

List of Figures

List of Tables

Chapter 1

Introduction

In recent times main source of energy in world is fossil fuels. Since the last decade there has been unprecedent increase in its usage. Being a non renewable source of energy its resources are facing a grave threat of depletion. This global demand of energy as well as the environmental effects of the hydrocarbons based power sources has led to the need for an alternative and renewable source of energy.

1.1 Renewable and Non-Renewable Energy Sources

Energy sources can be broadly classified as renewable and non renewable. Energy obtained from sources which can be replenished easily comes under renewable energy such as solar, wind, geothermal, tidal energy whereas conventional energy sources which are exhaustible and cannot be replenished easily like fossil fuels are non renewable energy sources[16].

Lately there has been tremendous increase in the energy requirements of the world because of the population increment, industrilization and modernization. According to the latest report by BP Statistical Review of World Energy 2017 there is 1% increase in consumption of global primary fuel in year 2016, following the 0.9% growth in 2015 and 1% in 2014. As compared to the 10-year average of 1.8% a year[1].

In presented report it is clear that fossil fuels have major dominance over the renewable energy sources as its contribution is 11946.4 mtoe whereas later having the consumption of 1329.9 mtoe which is nearly 4% of the total as shown in Fig1.1.

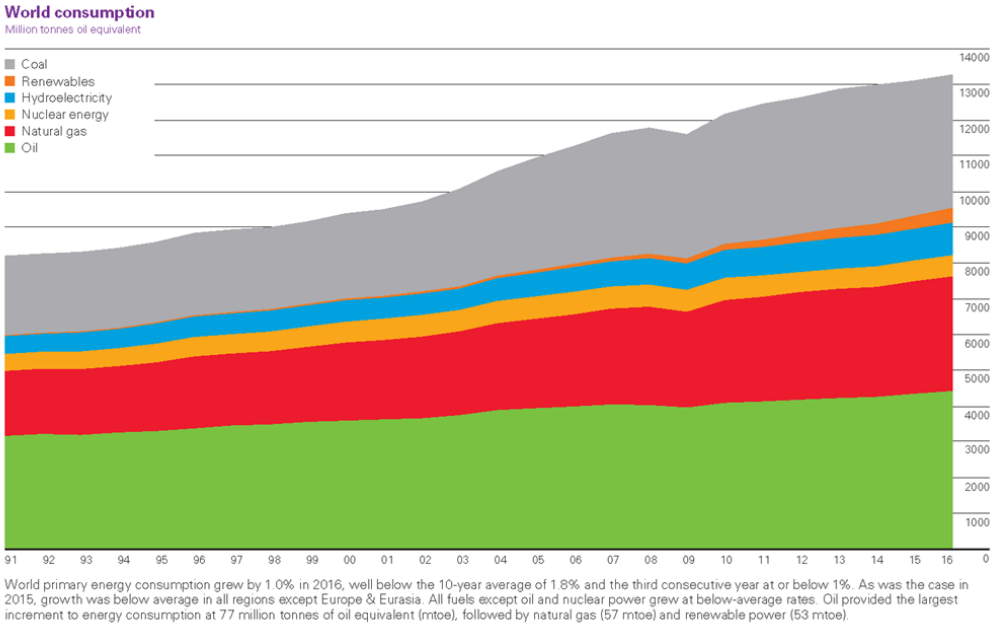

Figure 1.1: World Energy Consumption Growth Graph[1]

Also the growth in supply and production is lagging behind the consumption [17]. This indicates that sooner or later the reserves of the natural resources will be depleted. So, there is need to focus towards the growth of renewable resources. Among many renewable resources solar energy is the good alternative to the depleting fossil fuels as it is inexhaustible and abundant in nature.

1.2 Solar Energy and its Application

Solar energy is the one of the everlasting source of energy. The amount of solar radiation reaches earth atmosphere is around 1361 W/m^2.The electromagnetic spectrum of total solar irradiance is similar in shape to that of blackbody nearly at 6000^{o}C (as shown in Fig 1.2) which consists of large wavelengths ranging from infrared to visible and ultravioletto X-rays[2]. Some part of this energy is absorbed by the gases in atmosphere and re-radiated to the surface of earth in the mid infrared and far infrared wavelength while rest of the energy is absorbed by the surface or the organic life is re-radiated. The 99% energy of this solar spectrum is made up of near ultraviolet,visible and near infrared regions in the wavelength range of 0.15 to 4 μm[18].

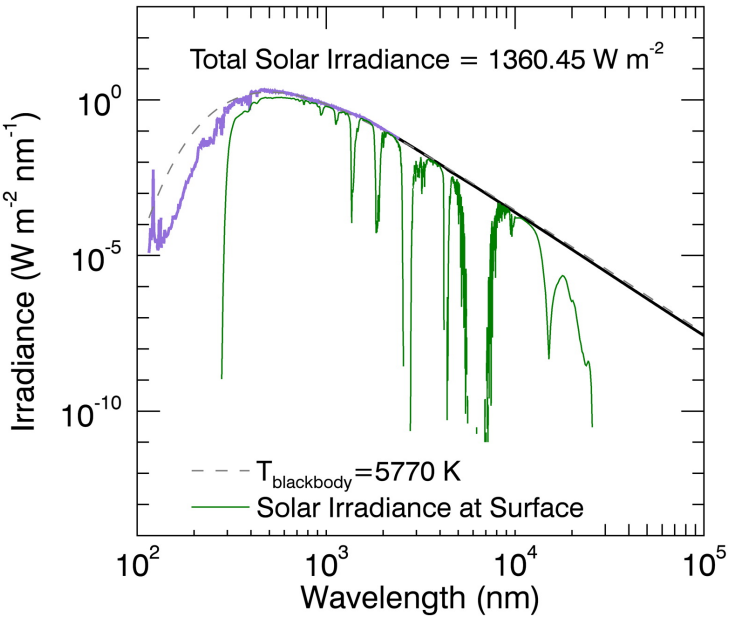

Figure 1.2: Electromagnetic Spectrum of Solar Radiation on log-log scale[2]

Out of this 52% consists of infrared, approx 39% visible light(400 nm $< \lambda <$ 700 nm) and less than 9% of ultraviolet ($\lambda <$ 400 nm). This energy when absorbed by any object on earth is converted to heat[19].

1.2.1 Solar Cells

Being abundant in nature there is lot of research going on in the field of solar energy harvesting for the production of electricity. First photovoltaic (PV) cell was developed in early 1950s since then lot of advancement has been made in this field. The PV cells are made up of semi-conductor material which are used to convert sunlight to electricity directly. But still it cannot be utilised to its full potential as current PV technologies do not have good efficiency. They have limited efficiency of around 30% which is due to the band gap of the material used. Also they require the mechanical tracking for normal incidence of sun rays, they don't work at night or during the unclear weather.

1.3 Proposed Solar Energy Harvesting Technique

New techniques are under research so as to achieve high efficiency and make solar harvesting cheaper. Among these techniques, nanoantenna is one method that can be used to replace the existing solar cells. By placing the rectifier within the antenna arms a rectifying antenna can be formed which utilize the wave nature of light and gives rectified AC as the output.

1.3.1 Rectenna

The use of nanoantenna for energy harvesting is the innovative and efficient alternative method. The proposed research aims to use the nanoantenna in IR region as IR energy is abundant in nature, since the traditional solar cells utilizes only the visible range of the solar spectrum.

When antenna is coupled with the rectifier it forms a rectenna i.e. a rectifying antenna. A rectenna is a combination of a antenna and a diode. Theortically these structures have no efficiency limits as there is no band gap problem as present in semiconductor. When there is perfect matching between the diode and antenna and efficient rectification is present then rectenna can have conversion efficiency upto 100% in optical region whereas 90% efficiency in microwave region[7].

When rectenna is used in optical region it confines a higly localised field in their feed gap because of their ability to enhance the interaction of light with nanoscale objects. Antenna used in the rectenna circuit can be dipole, spiral, slot or bowtie[20].

Here in the Fig 1.3 basic block diagram of rectenna has been shown.Here low pass filter is used for impedance matching between the diode and the antenna. Also it prevents reflected wave from the diode to antenna. At end of the diode pulsating DC is obatined as the output which when passed through DC Pass filter give a pure DC[3].

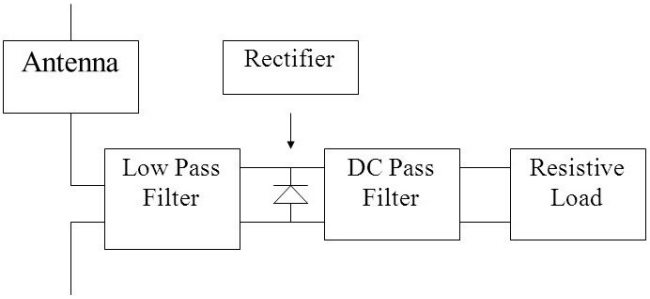

Figure 1.3: Block diagram of Rectenna[3]

Compared to PV cells, nanoantenna based energy harvesting has an upper hand due to its ability of operation during night and its independence of the atmospheric constraints such as humidity, rain etc. On top of that, they need not to have a particular orientation for the collection of energy as their radiation pattern is almost isotropic in nature, which is not the case with solar cells. Also they can harvest energy from the waste heat generated by the industries in the form of IR. In the below Table 1.1. comparison between the solar cells and the rectenna has been shown.

Parameters	Solar Cells	Rectenna
Operational Duration	During daytime only	Whole day and night
Weather Condition	Requires dry and clear weather	Works under all weather conditions
Orientation	Should always be facing the sun	Less sensitive to orientation
Cost	High	Low
Efficiency	High	Low
Waste Energy Harvesting	No	Yes

Table 1.1: Comparison of Solar Cells and Rectenna

1.4 Objective of Thesis

- Theoratical study of surface plasmons and localised surface plasmons on the metal-dielectric interface.
- Design of nanoantenna to resonate at 75.6 THz with greater enhancement in the electric field intensity than the existing nanoantennas.
- Design of MIM diode to work as rectifier at THz range.
- Coupling the nanoantenna and the MIM diode.
- Study the characteristics of the nanorectenna.

1.5 Contribution

The objective of this project is to design a efficient inexpensive solar energy harvesting nanoantenna.The contribution of this project can be summarised as follows.

- Designing a polarization independent nanoantenna
- Optimization of designed nanoantenna.
- Analysis of the array structure of the nanoantennas
- Theortical study of the characterisitics of the designed diode.
- Designing of the nanorectenna device which produces rectified AC without any external source of energy

1.6 Thesis Outline

The thesis have been organised as follows:

- Chapter 2 gives the glimpses of the background history of the rectennas. In addition to this, existing nanoantenna and MIM devices have been discussed.
- Chapter 3 gives the details of electromagnetic theory with analysis of surface plasmons and their role in the functionality of optical antenna.

- Chapter 4 gives the concept of design considerations for optical antennas and comparison of different types of antenna. Along with the design and optimization of Shuriken shaped nanoantennas for field enhancement have been discussed.
- Chapter 5 discusses about the theory of tunnel diode such as operation and basic properties. Also the characteristic analysis of the nanorectenna is presented.
- Finally,last chapter discusses about the future aspects of the work and the conclusion

Chapter 2

History of Rectenna and Review of Existing Devices

Energy harvesting through nanoantenna is a novel concept and much work has not been done in this regard.Nanorectenna is still under research.In this chapter history of the rectenna and its evolution through time has been discussed.Along with this development of various nanoantennas and MIM diodes have also been studied.

2.1 Historical Background of Rectenna

Idea of wireless power transmission goes back to the work of Hertz and Tesla.Tesla experimented with the gaint coil and 3-ft diameter copper ball to transport the low frequency EM wave from one place to another.This work further led to the new ideas of wireless power transmission in the field of microwave.The inital concept of rectenna was put forward by the person named William C. Brown who was later hailed as the father of microwave power transmission.In year 1964 he demonstrated the wireless transmission of the electricity in which he powered the helicopter with help of rectenna that converts the incoming microwave beam at 2.4 GHz into DC energy which is shown in Fig 2.1. This marks the begining of energy harvesting through antennas[4].

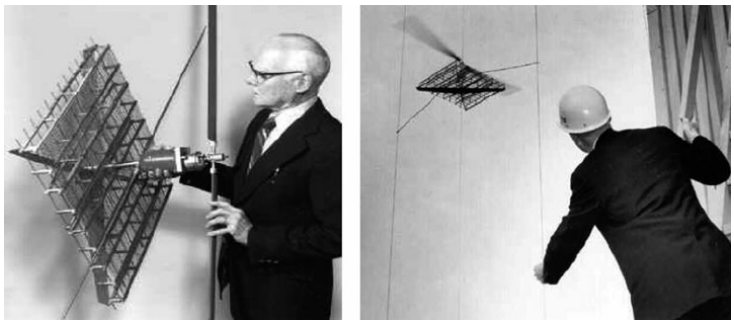

Figure 2.1: William C. Brown with rectenna powered helicopter[4]

Brown in his experiment used array of 28 half-wave dipole antenna that gives 40% to 70% of efficiency. He placed the elements in the form of brigde network in different combinations such as parallel, series and combination of parallel-series using the metal semi conductor diode at the junction with the recieving antenna. In order to form the microwave beam he used horn antenna whose feed point was connected to the transmission line as shown in Fig.2.2[5].

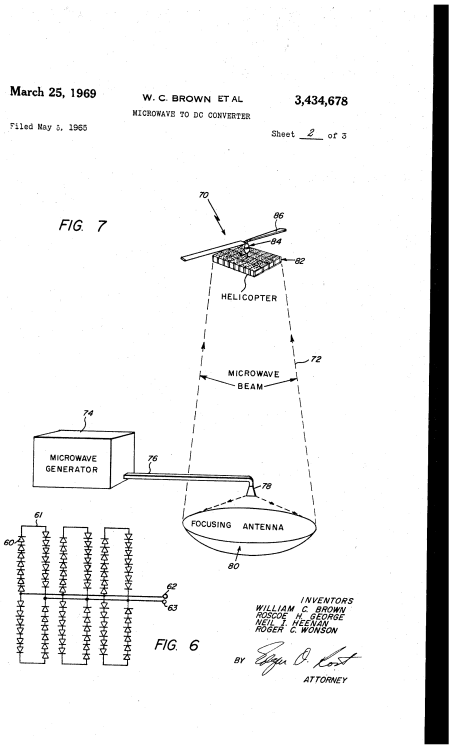

Figure 2.2: Structure of Brown's Rectenna powered helicopter[5]

As Brown introduced the concept of rectenna, Bailey was the first to utilise this in the solar energy harvesting. He proposed the idea of solar energy harvesting using rectenna in 1972 according to which the incoming solar radiation could be converted to electricity by using rectenna. Here he used the conical or pyramidal elements which has been obtained by modifiying the existing dipole antenna and then half wave rectifier is attached to it which generates the DC this is shown in Fig 2.3. Efficiency was around 12%-13% with centre frequency at 475 MHz and pass band at 200-700 MHz[6].

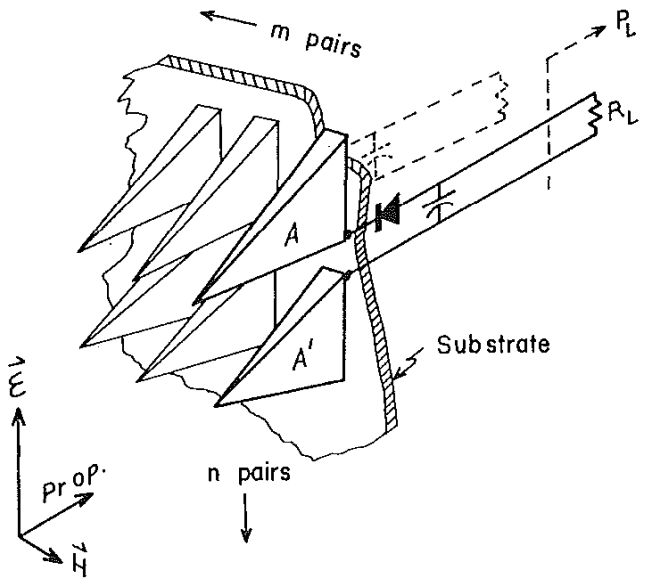

Figure 2.3: Design of Electromagnetic energy converter given by R.L.Bailey [6]

In 1984 another researcher Marks designed a rectenna using the array of crossed dipoles. This design has the theoretical efficiency of 67%. He used array of dipoles antenna in conjunction with rectifier made of Si. Dipole has its length and width in nanometer because of which device was working in range of near UV to Near IR. Marks design was significantly different from that of Bailey's, as former used the broadside antenna array in which the ouput signal from multiple dipole were feed to transmission line and then rectified. Also, the device was working in wavelength range of 0.35μm to 0.8μm. More research was conducted by Marks in this regard where he made devices of oriented molecular dipoles contained in solidified sheets. Also he invented a Femto diode in 1988 with which he was able to achieve a theoretical efficiency of 90% in range of visible light[7]. He also used a chain of iodine

molecule as conducting elements. However all the work done by him was never measured and he also ignored the calculation of antenna and rectifier mismatch which is one of the important aspects in the design and fabrication of the rectenna devices.

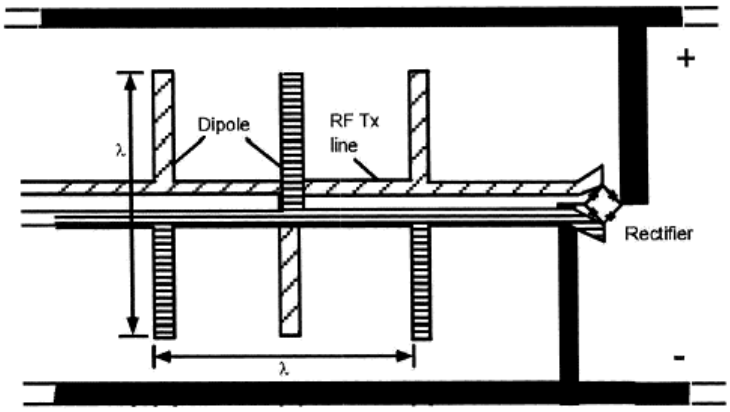

Figure 2.4: Marks Design of Rectenna using Crossed Dipole antenna[7]

Moving further in 1996 Lin et al. were the first to work towards the metallic nanostructures at THz frequency. In their design they have used array of parallel dipoles with Si as substrate and a pn junction diode as rectifier[21].

2.2 Microwave Rectenna Vs Optical Rectenna

When rectenna were invented they were working in the microwave range later on as more and more application of rectenna came forward working range of rectenna shifted towards the optical region. Microwave rectenna went under lot of research to improve its working efficiency. In 1992, McSpadden et al. investigated the rectenna made up of microstrip test mount with GaAs schottky barrier diode for microwave power transmission at 2.45 GHz and 35 GHz whose measured efficiency was 85% and 29% respectively[22]. In 2002,Suho et al. developed a dual frquency printed dipole rectenna whose measured efficiency was 84.4 and 82.7% at frequency of 2.45 and 5.85 GHz respectively[23]. Similarly in 2001 Bernal et al. of ITN Energy Systems Inc. proposed a infrared rectenna for conversion of solar energy into electricity. They developed rectenna of array of dipole antenna and schottky diode to operate at 10GHz. They obtained the conversion efficiency of $> 50\%$[24]. In 2008 Kotter et al. developed the solar nantenna electromagnetic collector with sipral nanoantenna to work in mid infrared wavelength. The designing

and fabrication of rectenna at microwave range does not pose much difficulty as their Optical counterpart where impedance matching between antenna and diode is big challenge[25].

2.3 Optical Nanoantennas

Optical antenna was invented because of its need in microscopy irrespective of its microwave counterpart whose major application is in the field of communication.

Optical antenna is generally defined as a device that convert free propagating optical radiation to localized energy, and vice versa. As more research has been conducted in this field it is found that optical antennas have their application not only in the microscopy but also in photovolatics, spectrocopy, nanoscale imaging, light emission and coherent control[26]. Generally metallic nanoantenna is used for photovoltaic application as it generates highly localised electric field at its feed due to the generation of localised surface plasmon which is used as input to the rectifier. This gives the DC current as the output[20].

In this work, energy harvesting has been achieved using plasmonic nanoantenna. Hence it is important to discuss their innovation through time. In 1985 Yasuko has given the idea of IR rectenna. Rectenna was made up of thin film antenna and Schottky diode,working at 10.6 μm.

In 1996, Lin et al. were first to experimentally observe a nanoantenna working in visible range. They have used parallel dipole antenna array as their nanostructure and boron doped p-type Si as its substrate. They observed that resonance peak is occuring when the polarization of incident light is parallel to that of antenna. Also the signal peak was observed at photon energies smaller than the Si band gap energy, which shows the absorption and rectification[21].

In 2000 Kottmann et al. studied the plasmon resonance in irregular shaped nanostructures for high electric field enchancement. Comparison between regular and irregular shapes have been done to verify the electric field enhancement[8]. It has been shown that isosceles triangle of base 10 nm has less enhancement to that of 20 nm right angled traingle having base of 10 nm for same incident wavelength of 365 nm. Here in the below Fig 2.5 field enhancement is shown for right angle triangle of 20 nm having base 10 nm.

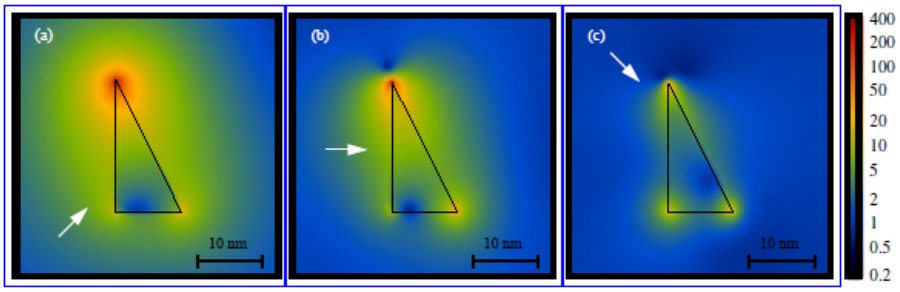

Figure 2.5: Electric Field intensity of right angle triangle of 20 nm having base 10 nm for (a) $\lambda = 458$ nm, (b) $\lambda = 392$ nm, (c) $\lambda = 364$ nm[8]

In 2005, Sundaramurthy and Crozier theoretically and experimentally studied the electric field enchanement in the gap of bow tie antenna. Each side of Au bow tie antenna is of 88 nm and the radius of curvature of the tip is 12 nm. The gap between the triangles is varied from 16 nm to 500 nm. It has been observed that when there is gap of 16 nm near field intensity of electric field is 1645 times relative to the incident beam. They also observed the current distribution along the antenna axis and measured the displacement current density for different gaps[27].

In 2008, Fischer et al. studied the optical properties of plasmonic dipole and bow tie antenna using the Green's Tensor Technique. Gold dipole and bow tie antenna of thickness 40 nm is made. Dipole has width of 40 nm whereas width of apex in bowtie is 20 nm. After the gap, length, bow angle optimization of bowtie and dipole antenna it was observed that dipole has more electric field enhancement as compared to bow tie antenna under same parameters[28].

In 2010,Kotter et al fabricated a nantenna electromagnetic collector for efficient energy harvesting. Here double feed point square spiral nantenna element had been designed and fabricated over Si substrate to operate at a wavelength of 6.5 μm. Spectral response of the device from 3 μm to 15 μm has been investigated using spectral radiometer and FTIR analysis method[9]. It has been observed that antenna used here can absorb upto 90% of the in-band energy. Also efficient method of roll-to-roll manufacturing the nanostrcture has been suggested as shown in Fig 2.6

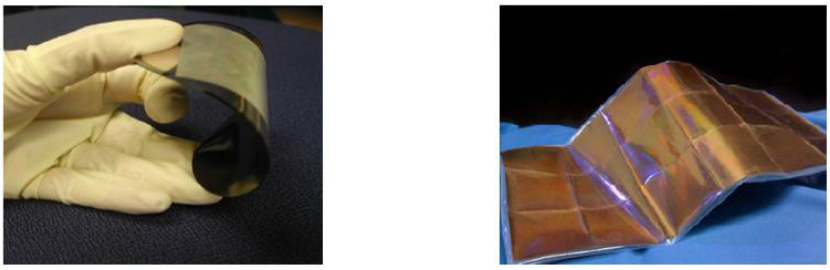

Figure 2.6: Roll-to-roll manufacturing method of nanostructures[9]

In 2011, Zhu et al. have reported a top down fabrication method to fabricate a pair of nano dimer separated by a small gap size. Array of dimers are made of gold where everyone of them are 100 nm long, 80 nm wide and 30 nm thick as shown in Fig 2.7.

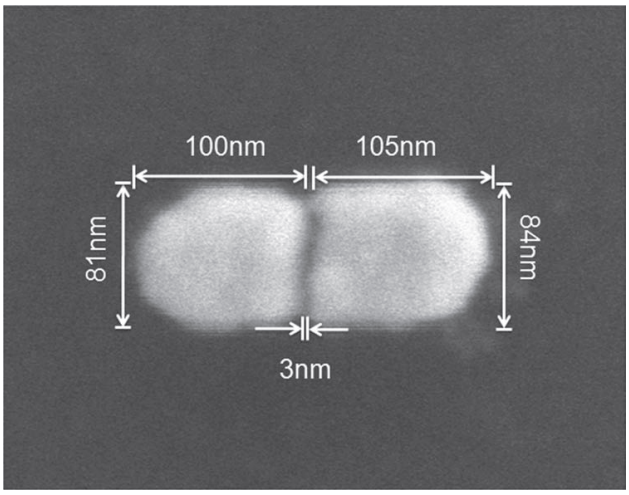

Figure 2.7: Gold Nano Dimers[10]

Outer edge of the nanoparticle is rounded with radius of 40 nm. Here the gap size could be reduced upto 10 nm and high enhancement factors of Surface-enhanced Raman scattering (SERS) had been observed. With gap size of 10 nm electric field enhancement factor(EF) is $\approx 10^7$ due to the interaction of localised surface plasmon resonance of each nanoparticle. When gap size is reduced to 5 nm or below EF can be $\approx 10^8$ or more[10].

In 2012, Thorsten Feichtner deviced a evoutionary algorithm to find the new antenna geometry by optimizing the near field intensity enhancement. The designed antenna is a hybrid of split ring and two wire antenna as shown in Fig 2.8[11]. Field is enhanced by the factor of 2 as compared to fundamental split ring and dipole antenna.

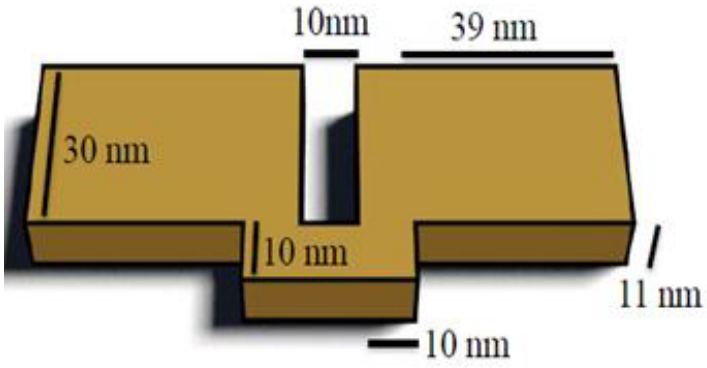

Figure 2.8: Hybrid structure of split ring and two wire antenna[11]

A new idea of collection of high intensity electric field at a point away from array of antenna was presented by Sabaawi in 2013[12]. A array 2x4 of gold bowtie antenna is constructed and feed lines are connected through each antenna as shown in Fig 2.9.

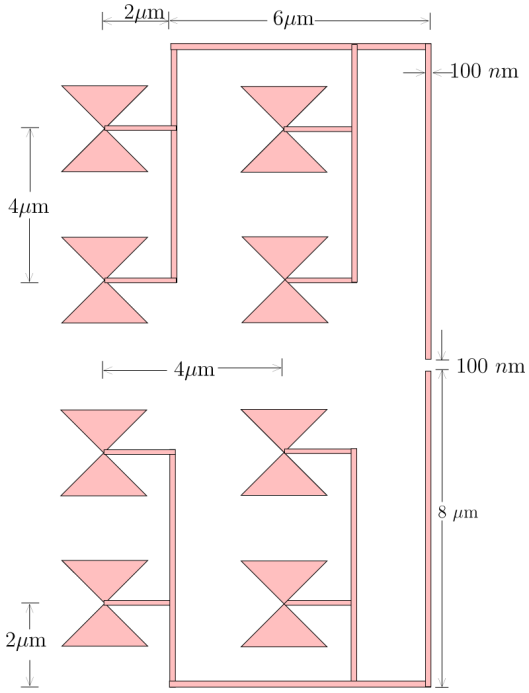

Figure 2.9: Configuration of Bowtie nanoantenna array[12]

These feed lines then transfer the captured electric field away from the

centre of antenna. At first resonant wavelength of 20.5 μm electric field of 0.047 V/μm and 0.258 V/μm at second resonant wavelength of 20.5 μm is obtained.

In 2014, Gadalla et al. presented a work in which they have used bowtie nanoantenna for energy harvesting in IR range. They have made two arms of bowtie antenna of gold and copper respectively and overlapping has been between that two arms. High electric field intensity of order 8 has been obatined at the resonant wavelength of 10.6 μm when gap size between the antenna arm is in between 0.5-1 nm[29].

2.4 MIM Diode

Normal diode can perform rectification but they cannot track a terahertz signal. Thus, for rectification of infrared signals tunneling effect is necessary. Hence a diode which works on the principle of quantum tunneling is used for the rectification purpose in nanorectenna. Tunneling occurs when the electron can pass through a thin layer of oxide. This effect cannot takes place when the thickness of insulator is more than few tens of angstroms as there is exponential decrease in the tunneling probability with increase in thickness of barrier. Sommerfed and Bethe were among first few people to study the tunnelling mechanisms[30]. They provided the equations for tunnelling current in case of rectangular barrier for very high and very low voltage. Equations for intermediate voltage case was given by Holm[31]. Both of them used the WKB approximation for deriving the current equations. First tunneling diode was fabricated by Fisher and Giaever in 1961[32]. They used Al electrodes and in between them aluminium oxide of 5nm thickness was placed. With the help of applied voltage and oxide thickness they were able to measure current and resistance variations. Simmons in 1963 put forward the theory which can be applicable to barrier of any shape[33]. Equations for the low and intermediate voltage for rectangular barrier is given as follows which are in the interest of this thesis.

Case 1: Low Voltage

$$J = \frac{3(2m\phi)^{\frac{1}{2}}}{2s}(\frac{e}{h})^2 V exp((\frac{-4\pi s}{h}(2m\phi_o)^{\frac{1}{2}})) \tag{2.1}$$

Case 2: Intermediate Voltage

$$J = \frac{e}{2\pi hs^2}\{(\phi - \frac{eV}{2})exp((\frac{-4\pi s}{h})(2m)^{\frac{1}{2}}(\phi - \frac{eV}{2})) - (\phi + \frac{eV}{2}) \\ exp((\frac{-4\pi s}{h})(2m)^{\frac{1}{2}}(\phi + \frac{eV}{2}))\} \tag{2.2}$$

where m is electron mass, e is charge on the electron, h is Planck's constant, s is thickness of barrier, V is applied voltage, ϕ_o is barrier height and J is tunneling current density. Two conclusions can be drawn from above firstly, there is exponential decrease in current density with increase in oxide thickness. Second, for the tunneling of electron there should be difference in work function of the two metals.

Initial MIM diode that were fabricated were traditional point contact diode.These were called as "cat-whisker diode". In these diode metal plate is pressed with a W wire to form a tunnelling junction as shown in Fig 2.10. They were initially used for the detection of microwave and frequency mixing of milimetre wave.

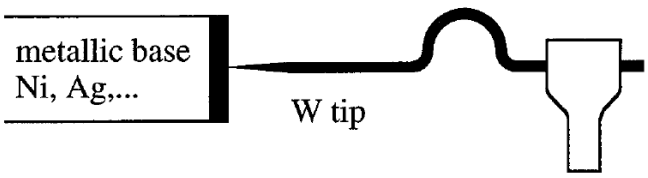

Figure 2.10: Diagram of point contact diode

Disadvantage of point contact MIM diode was its fabrication and the fabricated diode were fragile. In 1968, Hocker[34] made a point contact diode whose operational frequency was 337μm,until that time these diode have their application in millimetre range only. When Gustafson and Bachner[35][36] in 1974 fabricated a planar MOM diode using two thin strips of metal as shown in Fig 2.11, the problem of reproducibility was removed.

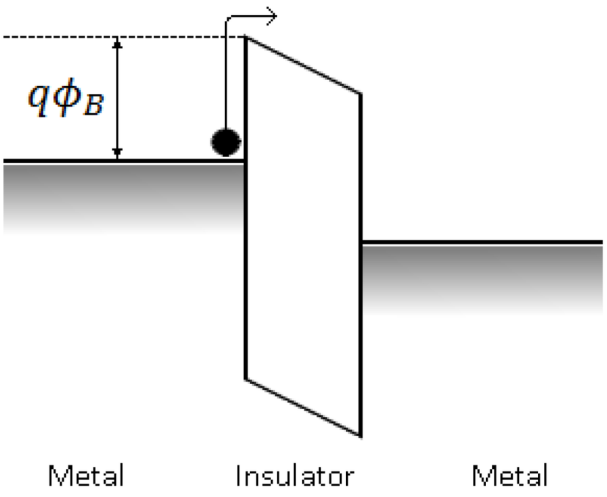

Figure 2.11: Planar Metal Oxide Metal Diode

In this thesis planar MIM diode is used with nanoantenna for rectification purpose.Here some already fabricated MIM diode has been discussed. C. Fumeaux in 1997 made the smallest thin film MOM diode. $Ni-NiO-Ni$ diode with area of 0.012 μm^2 is integrated with the bowtie antenna[37]. It is used for the detection of IR as well as mixing of difference frequencies upto 85 MHz.

Research in the field of MIM diode has progressed slowly as compared to the nanoantenna. $Ni - NiO - Cr$ MIM diode having the contact area of 1.45 $\mu m^2$was fabricated by Krishnan et al in 2006[38]. This diode was asymmteric, nonlinear and planar having its cut-off frequency of 0.1THz.

In 2010 Periasamy et al. fabricated a point contact MIM diode based on $Nb - Nb_2O_5$ and $Nb - TiO_2$ having small contact area[39]. These diode exhibits good asymmetry and nonlinearity with low turn-on voltage. Zero bias response with zero bias sensitivity is very critical to the solar energy collector application. This can be achieved only when diode is fabricated of two metals having different work functions. As at zero bias it will lead to fermi level gradient which promotes the electron tunnelling.

2.5 Summary Of Different Types of MIM diodes

Reference	**Type of MIM Diode**	**Maximum sensitivity (V^{-1})**	**Zero Bias sensitivity (V^{-1})**	**Zero Bias resistance (ohm)**	**Oxide Thick-ness(nm)**
Twu(1974)	Point contact diode of W and Au	3	-	-	unknown
I,Wilke, et al.(1994)	Ni-NiO-Ni (0.0576 μm^2)	1.6	-	100	4
Abdel-Rahman et al.(2004)	Thin flim Ni-NiO-Ni ($0.075\mu m^2$)	2.75	-	180	3.5
Esfandiari (2005)	Thin film Ni-NiO-Pt ($0.0025\mu m^2$)	-13	-3	-	2
S.Krishnan et al.(2008)	Ni-NiO-Cr/Au ($1.45\mu m^2$)	5	1	500K	3

Dagenais et al.(2010)	thin film polysilicon-$SiO_2 - Au$ ($0.35\mu m^2$)	-14.5	2.5	120 M	60
Beamn et al.(2011)	Thin film Al/AlOx/Pt ($0.5625\mu m^2$)	-2.3	0.5	220K	0.6
Zhang et al.(2013)	Ni-NiO-Cu ($0.008\mu m^2$)	7.3	-	1.2M	2-12
Gadella et al.(2014)	Au-Cuo-CU ($0.0045\mu m^2$)	6	4	505	0.7

Table 2.1: Comparison of different types of MIM diodes

2.6 Nanoantenna Integrated Rectifier

Antenna integrated MIM diode model was given by Sanchez in 1978[13] as shown in Fig 2.12.

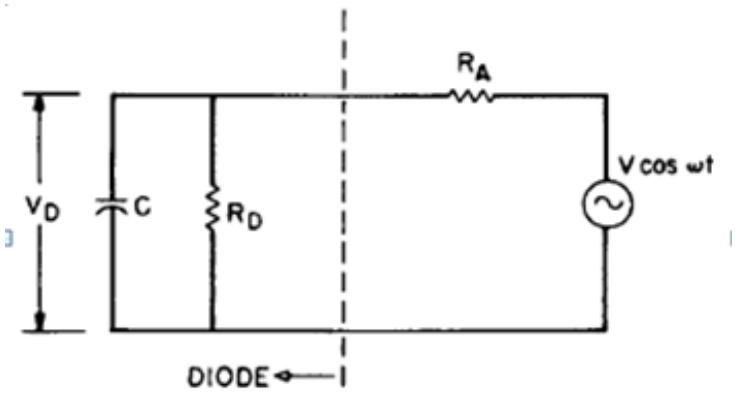

Figure 2.12: Equivalent Circuit Diagram of Antenna Integrated MIM diode [13]

In this figure ac source represents the antenna portion having an internal resistance of R_A while the nonlinear resistance R_D denotes the diode,in its parallel there is capacitance C which is present due to the contact of antenna and diode.

Whereas Hobbs [40], has given the conversion efficiency of the integrated system.Total conversion efficiency is given as follows

$$\eta = \eta_a \eta_s \eta_c \eta_j \tag{2.3}$$

η_a is coupling efficiency of em waves to the antenna, which is maximum at resonant wavelength of antenna. η_s is the efficiency of propogation and it represents the energy delivering ability of antenna to diode. It is less due to the material losses of antenna. η_j represents the conversion efficiency of diode. η_c is the efficiency of coupling between antenna and diode. As the diode resistance is usually higher than the antenna impedance to achieve good coupling efficiency is a major task. According to [41],[13]coupling efficiency is given as

$$\eta_c = \frac{4(R_A R_D/(R_A + R_D)^2)}{1 + \omega(R_A R_D/(R_A + R_D) C_D)^2} \tag{2.4}$$

After doing the literature review of various devices it is found that there are some drawbacks with them. In contrast with previous approach we can modifiy the antenna design such that firstly, it becomes polarisation independent. Secondly, it should be easy to fabricate. Also, the diode should be formed using the overlapping arms of the antenna and placing the oxide layer

in between them. So, designed diode can fully utilise the benefit of enhanced electric field intensity due to localised surface plasmon resonance.Because of this type of design antenna and diode mismatch can be reduced.

Chapter 3

Theory for Design of Nanoantenna and MIM Diode

In this chapter, electromagnetic theory and the basic concept of nanoantenna and MIM diode has been discussed along with the numerical technique used in the simulation of nanorectenna.

3.1 Electromagnetism

In 1873, J. C. Maxwell gave the basic equations of electromagnetics which explains the phenomenon of propogation, scattering and reflecton. Equations given by Maxwell were not experimentally explained. Hertz, in 1891, validated these equations through experiments. Electromagnetics is applicable from low frequency to high frequency till optical region.

3.1.1 Maxwell's Equations

Entire electromagnetism unfolds itself in the four Maxwell's equations which relate the electric and magnetic fields,continuity equation and the material related equations[42].These are given as follows:

Maxwell's Equations

$$\vec{\nabla} \times \vec{E} = \frac{-\partial \vec{B}}{\partial t} \tag{3.1}$$

$$\vec{\nabla} \times \vec{H} = \frac{\partial \vec{D}}{\partial t} + \vec{J} \tag{3.2}$$

$$\vec{\nabla} \cdot \vec{D} = \rho \tag{3.3}$$

$$\vec{\nabla} \cdot \vec{E} = 0 \tag{3.4}$$

Continuity Equation

$$\vec{\nabla} \cdot \vec{J} = \frac{-\partial \rho}{\partial t} \tag{3.5}$$

where $\nabla\times$ is the curl and $\nabla\cdot$ is divergence.
For isotropic and homogenous medium material equations are as follows

$$\vec{D} = \epsilon \vec{E} \tag{3.6}$$

$$\vec{B} = \mu \vec{H} \tag{3.7}$$

$$\vec{J} = \sigma \vec{E} \tag{3.8}$$

where,
$\vec{E}$ is electric field
$\vec{H}$ is magnetic field
$\vec{D}$ is electric flux density
$\vec{B}$ is magnetic flux density
$\vec{J}$ is current density
ρ is charge density
ϵ is the permittivity of medium
μ is medium's pemeability and
σ is conductivity

3.1.2 Boundary Condition For Electric and Magnetic Field

Whenever field exists in two different media,conditions which it has to satisfy at interface of the media are known as boundary conditions. These conditions depend upon the material of the media and they are obatined by using the Maxwell equations[42]. Electric and magnetic field boundary conditions are given as follows:
On the interface of two dielectric media:

$$D_{1n.} - D_{2n.} = \rho_s \tag{3.9}$$

$$E_{1t.} = E_{2t.} \tag{3.10}$$

$$B_{1n.} = B_{2n.} \tag{3.11}$$

$$(H_1 - H_2) \times a_{n12.} = K \tag{3.12}$$

where subscripts 1 & 2 indicate first and second medium and n & t represent normal and tangential component of different fields. When the medium is source free then $\rho = 0$ and K=0, then eqn.(3.9) and (3.12) can be written as

$$D_{1n.} - D_{2n.} = 0 \tag{3.13}$$

$$(H_{1.} - H_{2.}) \times a_{n12.} = 0 \tag{3.14}$$

When one media is perfect conductor then eqn.(3.10) and (3.11) changes to

$$E_{t.} = 0 \tag{3.15}$$

$$B_{n.} = 0 \tag{3.16}$$

3.1.3 Wave Equations

For isotropic homogenous and linear media wave equations are obatined using Maxwell equations[43]. Since Maxwell equations are coupled equations they cannot be directly used for solving boundary value problems. Firstly these equations are decoupled so as only one unknown value is present in the equation. The resultant equations are known as wave equation or *Helmholtz equation*. Using eqn.(3.1) and (3.2)

$$\nabla \times E = \frac{-\partial B}{\partial t.}, \tag{3.17}$$

$$\nabla \times H = \frac{\partial D}{\partial t.} + J, \tag{3.18}$$

By taking the curl on both side of (3.17)

$$\nabla \times \nabla \times E = \frac{-\partial}{\partial t.}(\nabla \times B) \tag{3.19}$$

Put J=0 and B=μH in eqn.(3.19) then put eqn.(3.18) in eqn.(3.19),then

$$\nabla \times \nabla \times E = -\mu\epsilon \frac{\partial^2 E}{\partial t.^2} \tag{3.20}$$

then using identity in eqn.(3.20)

$$\nabla \times \nabla \times F = \nabla(\nabla \cdot F) - \nabla^2 F \tag{3.21}$$

so,

$$\nabla(\nabla \cdot E) - \nabla^2 E = -\mu\epsilon \frac{\partial^2 E}{\partial t.^2} \tag{3.22}$$

then use ∇·E=0 in eqn.(3.22). So,

$$\nabla^2 E - \mu\epsilon \frac{\partial^2 E}{\partial t.^2} = 0 \tag{3.23}$$

This is wave equation for electric field.Similarly,wave equation for magnetic field can also be obtained which is given as follows,

$$\nabla^2 H - \mu\epsilon \frac{\partial^2 H}{\partial t.^2} = 0 \tag{3.24}$$

3.2 Antenna Theory

According to IEEE, antenna is a device for transmiting and receiving radio waves[44], hence antenna are reciprocal devices. Irrespective in which mode antenna is used its properties remain same.

For radiation in antenna there should be variation in current with time or acceleration of charge. If wire is bent, curved, terminated or discontinuous then there will be acceleration of charge. It is also created when there is oscillation of charge in time harmonic motion whose frequency can be given as

$$f_o = \frac{1}{2\pi\sqrt{LC}} \tag{3.25}$$

where L is inductance and C is capacitance of antenna. By changing the L and C antenna can be tuned to operate at different frequencies. For antenna to work in optical region L and C should be very small which can be obtained by scaling the antenna size w.r.t wavelength.

3.2.1 Radiation in Antenna

How radiation takes place in antenna has been discussed here. Assume a two parallel wire transmission line (TL). Moving charges create a traveling wave of equal current magnitude along each wire. These waves are reflected back from the end of the wire and superimpose on the incident wave resulting in the creation of a standing wave. Also, the current in each wire is 180^o out of phase. Radiation in antenna takes place due to the time variation of current and wire termination as shown in Fig 3.1.

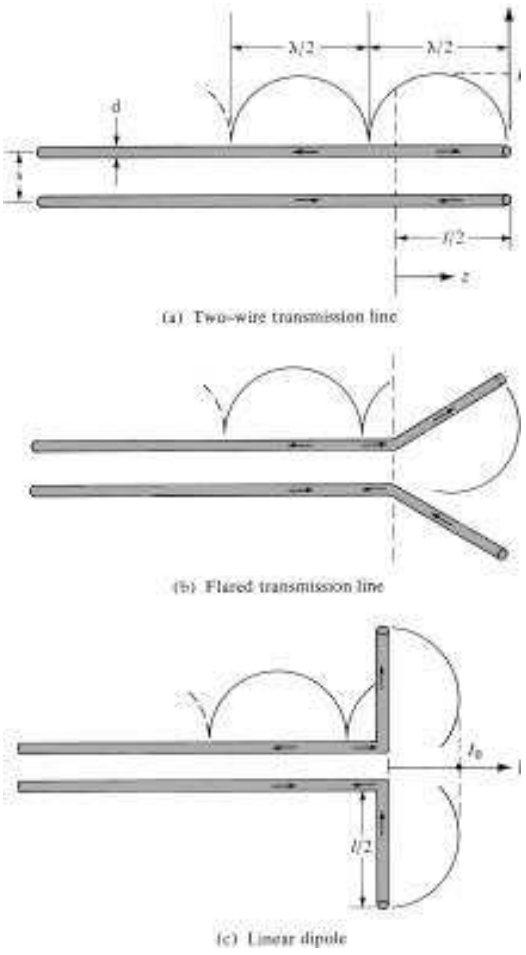

Figure 3.1: Current Distribution pattern in two wire transmission line

If the distance between the two wires is increased and wires are totally bend at 90^o then strongest radiation takes place and current distribution can

be given as [45]

$$I(z) = I_o sin(k(\frac{L}{2} - \mid z \mid)) \tag{3.26}$$

Reflection is caused due to the impedance mismatch between the impedance of antenna Z_a and characteristic impedance of TL, Z_o. Antenna impedance can be calculated as the ratio of voltage in feed point and the current of the antenna. It is given as follows $Z_a = R_a + iX_a$. where R_a is combination of load resistance and radiation resistance. Load resistance represents the power disipated in the form of heat and radiated power is given by radiation resistance.

$$R_a = R_r + R_l \tag{3.27}$$

Power radiated is given as

$$P_r = \frac{R_r}{2} I^2 \tag{3.28}$$

and radiation efficiency is given as,

$$\eta_r = \frac{R_r}{R_r + R_l} \tag{3.29}$$

Maximum power is transferred when there is matching between the antenna impedance and characteristic impedance of TL. Maximum power transfer occurs when $Z_o = Z_a^*$

3.3 Properties of Metal At Optical Frequency

When antenna is scaled down to work in optical region losses are increased which in turn affects its radiation efficiency. Whereas in Radio antennas, losses are trivial in matching circuits. Also the characteristics of nanoantenna depends upon the material and structure. These antennas can take any shape where surface plasmon resonance(SPR) plays an important role as at higher frequency metals does not behave as perfect conductor. The dielectric properties of metals become frequency dependent and are complex in nature.

In this section scaling, skin depth and dielectric properties of metals have been discussed.

3.3.1 Scaling and Skin depth

In conventional antennas wavelength λ plays an important role in the design of antenna. To use these antennas in optical region firstly they need to be scaled down. But wavelength scaling fails at THz frequencies as metals

behave as strongly coupled plasma due to the effect of skin depth. Distance upto which a field can penetrate a metal is known as skin depth. It is negligible in case of perfect conductor as it depends upon the conductivity and frequency. Skin depth is given as

$$\delta = \sqrt{\frac{2}{\omega\sigma\mu}} \tag{3.30}$$

But at THz frequencies skin depth has significant value because at high frequency metal does not behave as perfect conductor.

Generally length of antenna depends upon wavelength of input radiation as L =$\lambda\times$C where C is any constant value. But this scaling fails in the optical region as radiation penetrates the metal and interact with free electrons giving rise to the oscillations. So, at THz frequency nanoantenna responds to the effective wavelength(λ_{eff}) of the oscillations instead of λ of incident radiation.The λ_{eff} is shorter than that of incident. The λ_{eff} can be calculated as[46]:

$$\lambda_{eff} = n_1 + n_2\frac{\lambda}{\lambda_p} \tag{3.31}$$

Here λ_p is plasma wavelength, and n_1, n_2 are coefficients related to the design of antenna.So, the length of antenna will be $\lambda_{eff}/2$ which is shorter instead of $\lambda/2$.

3.3.2 Dielectric Properties Of Metal

At optical frequency metal behaves as dielectric and their dielectric properties becomes frequency dependent $\epsilon(\omega) = \epsilon'(\omega)+\iota\epsilon''(\omega)$.The permittivity of metal at optical frequency is given by Drude model.According to the Drude model

$$\epsilon_c = \epsilon_\infty - \frac{\omega_p^2}{\omega^2 + \omega_\tau^2} \tag{3.32}$$

where ω_p ,ω_τ are plasma frequency and damping or collision frequency respectively.These are the Drude parameters and have units of cm^{-1}. This equation can be separated into real and imaginary parts as follows

$$\epsilon' = \epsilon_\infty - \frac{\omega_p^2}{\omega^2 + \omega_\tau^2}, \tag{3.33}$$

$$\epsilon'' = \frac{\omega_p^2\omega_\tau}{\omega^3 + \omega\omega_\tau^2} \tag{3.34}$$

The imaginary part represents the ohmic losses which should be as low as possible.These losses are proportional to the conductivity $\sigma(\omega)$ which is relate to $\epsilon(\omega)$ as $\epsilon''(\omega) = \frac{\sigma(\omega)}{\epsilon_o(\omega)}$. By two methods, losses due to the material can be reduced in metallic nanostructures. Firstly, by choosing a metal with large real part which is negative in value. This will reduce the depth of penetration. Second,by reducing the ohmic losses by lowering the imaginary part i.e. $\epsilon''(\omega)$.

3.4 Surface Plasmon Resonance(SPR)

Metals consists of free electrons and fixed positive charges. These free electrons are in continuous random motion. So,high electron density appears at some place due to the repulsion and accumulation of electrons. This creates the charge oscillations as shown in Fig 3.2.

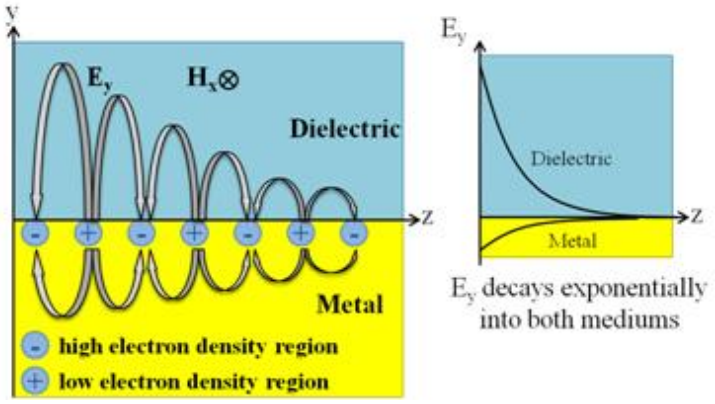

Figure 3.2: Formation of surface waves at metal dielectric interface

When light of certain wavelength ω is incident upon the metal plane it interacts with charge oscillation having wavelength ω_{sp}[47].

This is the case when $\tau^{-1} \leq \omega \leq \omega_p$ where ω_p is bulk plasma frequency, travelling wave appears on the interface of the metal and dielectric in perpendicular direction due to the resonance at the interface. This phenomenon of resonance is known as surface plasmon resonance whereas the EM excitation is known as surface plasmon polaritons (SPP). Waves on surface exist only when materials used are having permittivity (real part) of opposite signs. SPP only exists for Transverse Magnetic polarization. The dispersion relation for SPP is given as follows

$$\beta = k_o \sqrt{\frac{\epsilon_m \epsilon_d}{\epsilon_m + \epsilon_d}} \tag{3.35}$$

where β is propogation constant, k_o, is free space wave propogation vector, ϵ_m and ϵ_d is permittivity of dielectric and metal respectively.

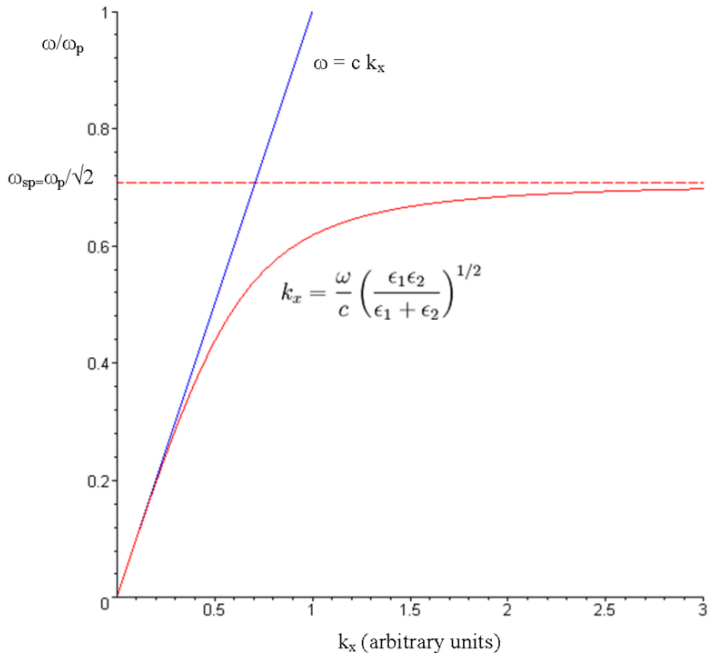

Figure 3.3: Dispersion relation of SPP at metal-dielectric interface

For large wave vectors frequency of surface plasmon polariton reaches the surface plasmon frequency given as

$$\omega_{sp} = \frac{\omega_p}{\sqrt{1+\epsilon_2}} \tag{3.36}$$

3.5 Localized Surface Plasmons

In previous section we have seen that SPP's are dispersive,propogating EM waves coupled to the e^- plasma of metal at interface.Here the concept of localised surafce plasmons resonance(LSPR) has been discusssed. Localized surafce plasmons are non propogating excitations. When the curved surface of the nanostructure exerts restoring force against the electrons, a resonance takes place. This resonance is called as LSPR[48].

Because of LSPR, energy is confined between edges of the finite shape nanoparticle. This confinement of energy leads to high electric field intensity at that point which can be used in many applications.

3.6 Application of Nanoantennas

Due to the ability to localize and enhance electric field at a point nanoantenna finds its application in various areas of optics. They are used in field of near field microscopy,spectroscopy,imaging and sensing, photovolatics, as optical sensors and switches. They are also used in the field of medicine.

Chapter 4

Design and Optimization Of Shuriken Shaped Nanoantenna

This chapter discusses the design considerations for the design and simulation of antennas. Also, the comparison of different types of nanoantenna and the effect of coupling two or more antenna elements in one strcuture has been studied.

4.1 Design Considerations

While the design of nanoantenna few design aspects should be taken in to account. These are operational frequency, structure and shape of antenna, material to be used for antenna and boundary conditions to be appiled. These aspects are discussed at length in following section.

4.1.1 Selection of Material

Material properties are different at RF and optical frequency because of which special attention should be given while the selection of material for antenna at optical frequency.Till radio frequency metal behaves as perfect conductor but when these antennas are scaled down to nanoscale properties of metal changes. In THz range metal exhibits characteristics of dielectric. They have low conductivity and their permittivity becomes frequency dependent. Their dielectric constant is complex in nature given as follows

$$\epsilon = \epsilon' + \iota\epsilon'' = N^2 = (n + \iota k)^2 \tag{4.1}$$

Here N is refractive index of the material.Because of skin depth the absorption in metal at THz frequency is higher than at the GHz range where it

is negligible. Ohmic losses in metal is given by ϵ'' which is related to the conductivity $\sigma(\omega)$. For substrate portion the material should be chosen such that the permitivity of metal and substrate have opposite sign.For the occurance of SPR metal should have high negative real part and subatrate should have positive permitivity. Drude model is used to characterise the dielectric properties of the metal at visible and Infrared region.

For designing antenna at IR and visible region several noble metals such as Gold, Silver, Copper, Nickel and Aluminium are considered. It is found that Gold and copper are the best choice among different materials. Gold is chemically inert and get less oxidised as compared to others while Copper is highly conductive and have high negative real part of permitivity. When these two metals are used together they produce high electric field enhancement at the feed point of antenna. Permittivity of gold and copper is obatined using Drude model

$$\epsilon(\omega) = \epsilon_\infty - \frac{\omega_p^2}{\omega^2 - \iota\omega\omega_(\tau)} \tag{4.2}$$

The vaules of ω_p, ω_τ and ϵ_∞ are taken from Ordal et al[49][50]. In this work both gold and copper has been used together as material for antenna.The dielectric contants of Gold and Copper have been shown in graph in Fig

4.1.2 Structure and Shape of Nanoantenna

Nanoantenna has ability to confine the electric field in narrow region.When single nanoparticle is used it scatters energy but when the nanoparticle are coupled they confine the energy in small area. For the purpose of energy harvesting, structure of antenna should be such that its maximum energy is confined in small and high electric field enhancement is obtained. Several structure such as dipole, dimer, square spirals, Archimedean spirals, bow tie have been designed to work in IR region. Geometrical parameters of these antennas are varied and their effect on antenna performance has been studied.

Here the study of structure has been done in two parts.Firstly the study of simple design such as rod,dipole, bowtie has been done.For that purpose design parameters have been taken from the paper of Cubukcu et al.[14] and are replicated to study the merits and demerits of geometrical parameters on antenna performance.Second,a new design of nanoantenna has been proposed after the study of previous designs.This new antenna has the shape of Shuriken and incorporates the best properties of bowtie and dipole antennas.

4.1.3 Wavelength of Operation

The amount of solar radiation reaches earth atmosphere is around 1361 W/m^2.The electromagnetic spectrum of total solar irradiance is similar in shape to that of blackbody nearly at 6000^oC (as shown in Fig 1.2) which consists of large wavelengths ranging from infrared to visible and ultraviolet to X-rays[2]. Some part of this energy is absorbed by the gases in atmosphere and re-radiated to the surface of earth in the mid infrared and far infrared wavelength while rest of the energy is absorbed by the surface or the organic life is re-radiated. The 99% energy of this solar spectrum is made up of near ultraviolet,visible and near infrared regions in the wavelength range of 0.15 to 4 μm[18]. Out of this 52% consists of Infrared,approx 39% visible light(400 nm $< \lambda <$ 700 nm) and less than 9% of ultraviolet ($\lambda <$ 400 nm).This energy when absorbed by any object on earth is converted to heat[19]. Part of energy which is reradiate to the earth's surface lies in the range of 4-25μm.This range contains large amount of IR energy which is necessary for the photovolatics. So,in this work 2-6μm has been chosen as range of wavelength for operation of nanoantenna as energy harvester.

4.1.4 Simulation Software

In this work COMSOL Multiphysics® has been used as the simulation software. It is a FEM (finite element method) based software. COMSOL Multiphysics® uses FEM to solve Maxwell's equation for the boundary conditions of the geometry. In FEM analysis is done according to the following steps

- Dividing the geometry into small elements,
- Obtaining the equations for each element,
- Placing all the elements in region of solution,
- Solving all the obtained equations.

In this work, Copper-Gold nanoantenna has been placed on the silica substrate and light of intensity 1 V/m is incident vertically upon the antenna from the z axis. The incident light can be x or y or both xy polarised as geometry is polarization independent.

For designing in COMSOL Multiphysics following steps have to be followed:

- Defining the parameters of the model

- Designing the geometry
- Assigning the material to the geometry
- Specifiying the boundary conditions to be used and defining the excitation
- Forming the mesh in the structure
- If needed, give parametric sweep
- Solving the model
- Analysis of the solution

4.2 Comparison of Different Types of Antenna

Earlier it has been mentioned that different antenna design were replicated and their performance has been studied.All the simulations have been done in COMSOL Multiphysics.

4.2.1 Single and Coupled Nanorods

A gold nanorod of cross section area 40×40 nm^2 having edge radius of 20 nm is placed on silica substrate having refractive index of n = 1.46 as shown in Fig 4.1.

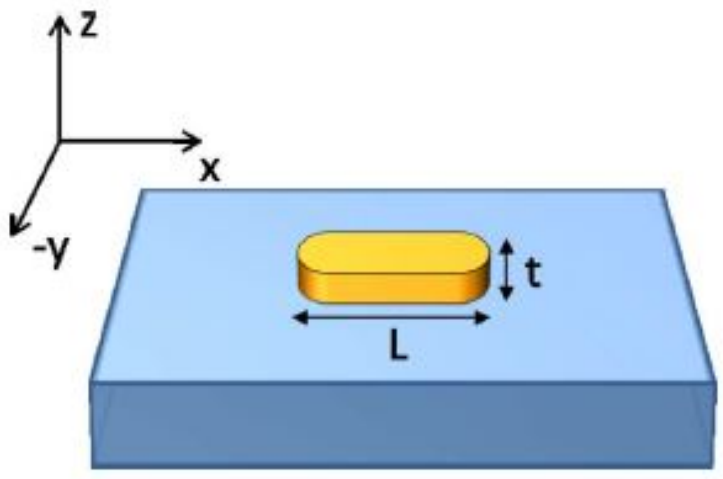

Figure 4.1: Design of Gold nanorod over Silica substrate[14]

The length of the rod is being varied to determine the maximum near field enhancement for a particular resonant length.During designing the scattering boundary condition has been used in every direction to avoid reflection. Light of 830 nm wavelength and E field magnitude of 1 V/m is incident upon the rod which is polarised along the antenna axis. It is observed that the first and second resonance occurs when the length of the rod is 150 nm and 525 nm and their near field intensity is nearly 600 and 460 times the intensity of incident light respectively, as shown in Fig 4.2.

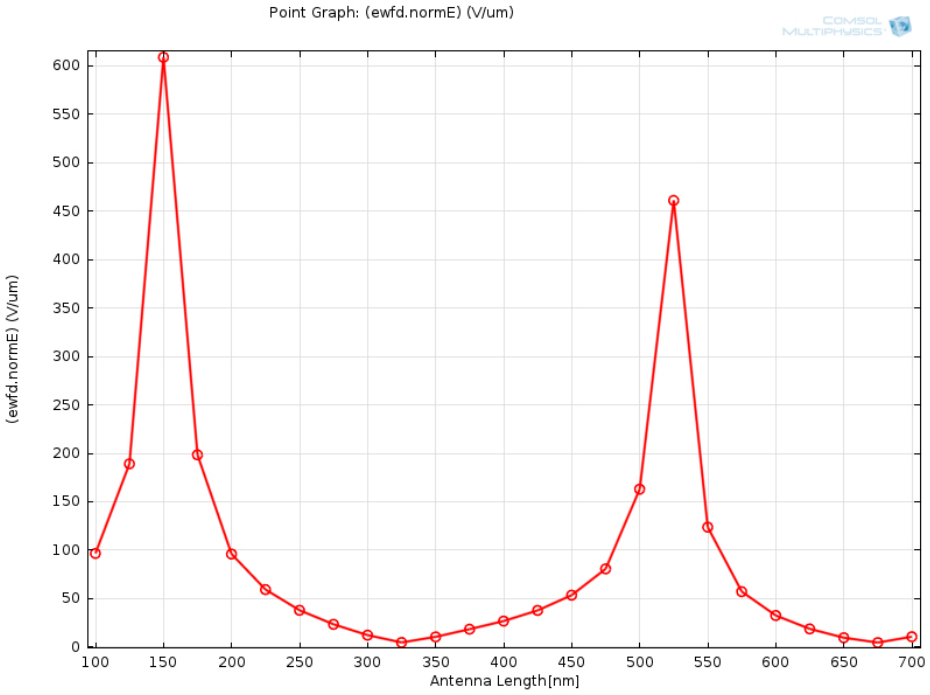

Figure 4.2: Electric field Vs Antenna length for single nanorod

Distribution of electric field amplitude near the nanorod which is x polarised has been shown in Fig 4.3.

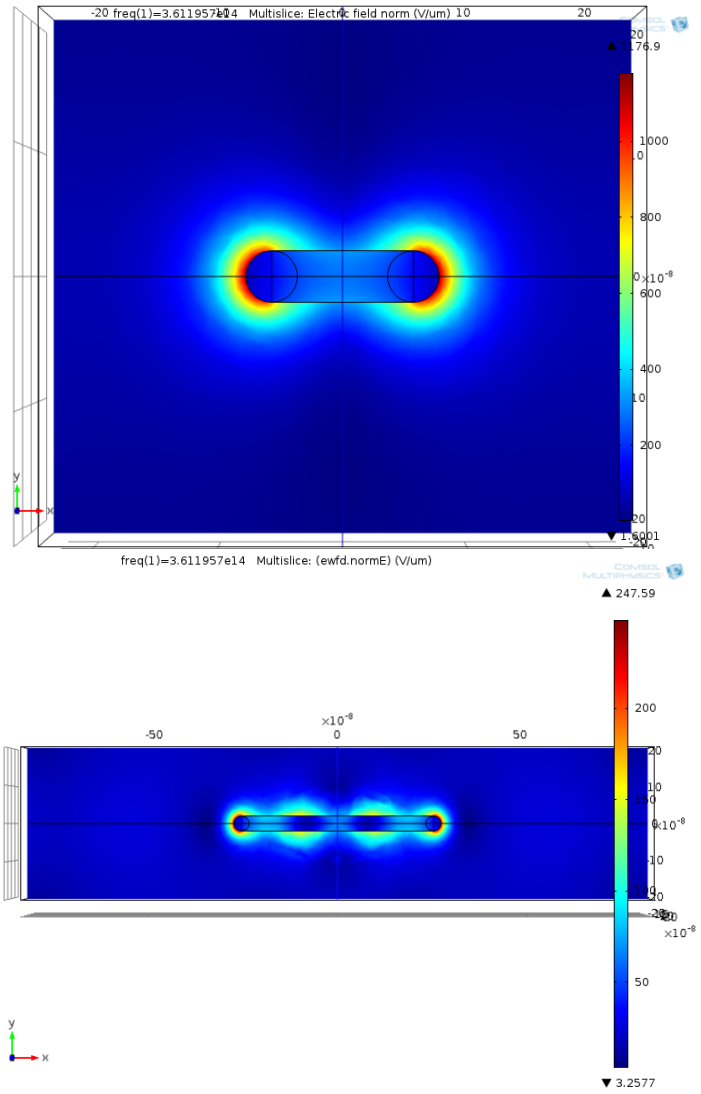

Figure 4.3: Electric field distribution around single nanorod of length 150 nm and 525 nm respectively

To observe more field intensity at the edges nanorods are coupled having the gap of 20 nm in between them as shown in Fig 4.4.

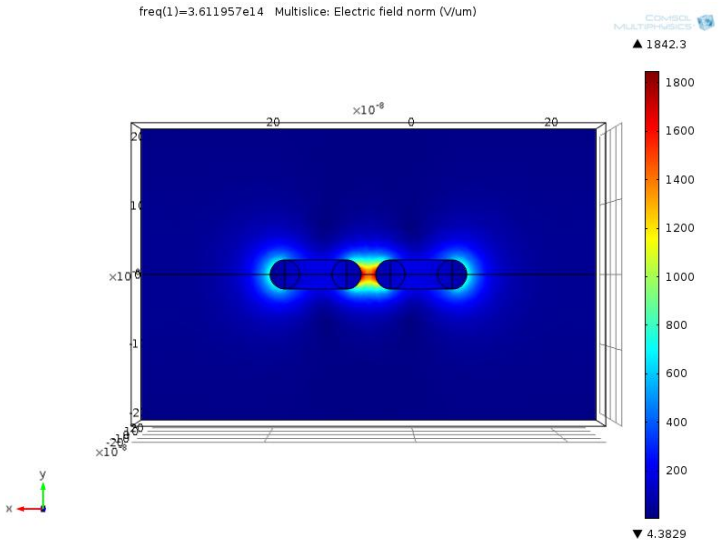

Figure 4.4: Electric Field Distribution in coupled nanorods when L=125 nm and gap = 20nm

Because of resonance between the two nanorod field has been increased 900 times than the incident field. Also the resonant length has been changed and now the first and second resonance is occuring at L = 125 nm and L= 500 nm. The field is mostly confined in the gap as shown in Fig 4.5.

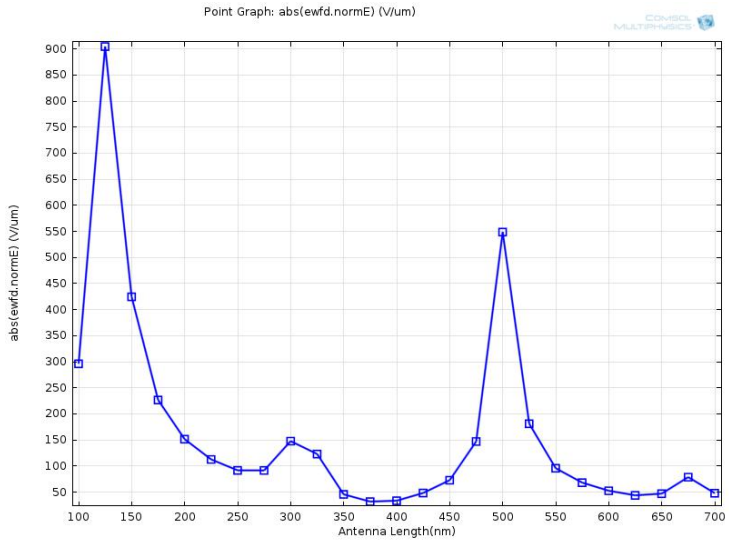

Figure 4.5: Electric field Enhancement at the gap and resonance peak at L = 125 nm and L = 500 nm

4.2.2 Triangular and Bow tie Antennas

Here simple triangular geometry has been analysed and observe the effect of sharp corner in the electric field enhancement. Like above this geometry is 40 nm thick and is placed on silica glass. X-polarised light having wavelength 830 nm has been incident along the axis of antenna. Antenna has flare angle of 60^o with edge having radius of 10 nm.

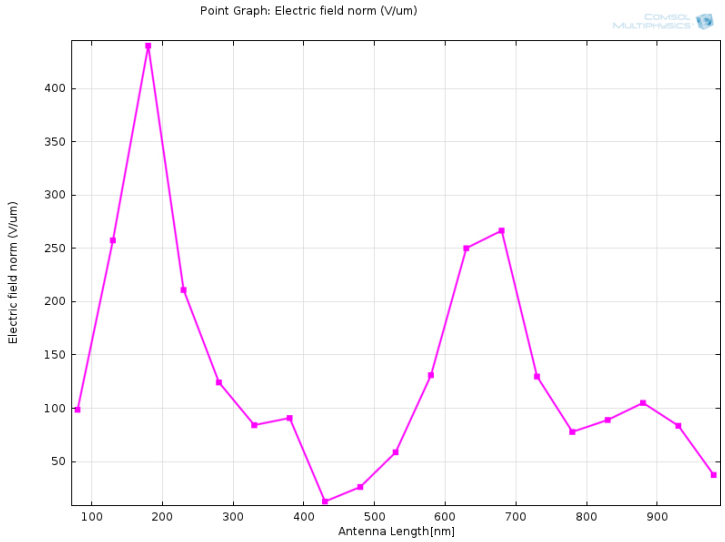

Figure 4.6: electric Field Vs Antenna length when the incident wavelength is 830 nm and is x polarised

Graph in Fig 4.6 shows that the resonance is occurring at the length of 180 nm and 680 nm and field enhancement corresponding to these length are 420 and 260 respectively. Since the conduction current flows from wide end to narrow end of antenna, the field is concentrated at the narrow edge of due to the lightning rod effect.The electric field distribution is as shown in Fig4.7

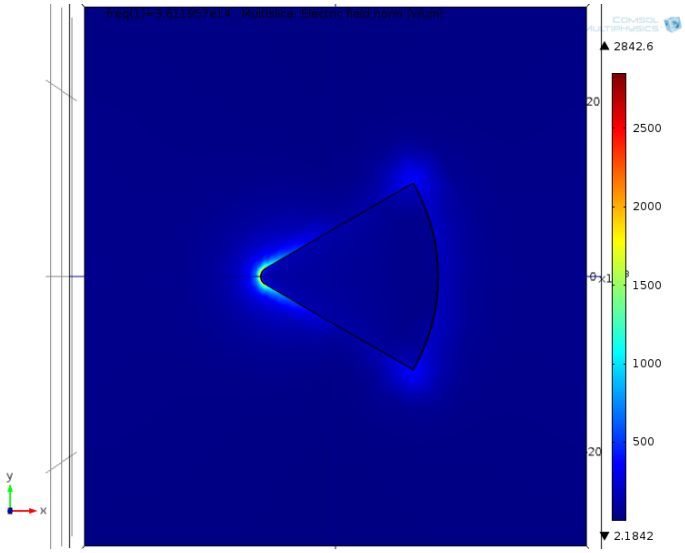

Figure 4.7: Electric field distribution around the triangular antenna when the L=180 nm

Whereas in coupled triangular antenna known as Bow tie antenna the electric field enhancement of 440 and 240 occurs at L = 140 nm and L = 720 nm respectively when the gap between the antenna arm is 20 nm. This is due to the dipolar resonance between the antenna arms which are interacting capacitively with each other. At L = 300 nm and L = 860 nm resonance peaks are appearing due to the quadrupolar resonance of single antenna arm as shown in Fig 4.8.

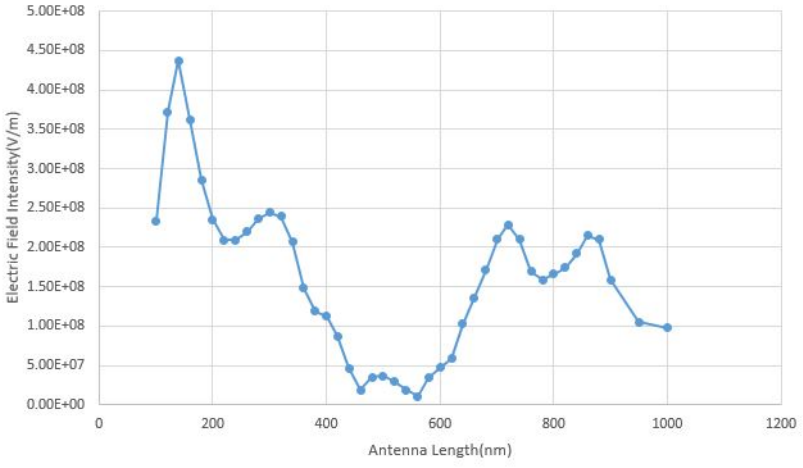

Figure 4.8: ELectric field Vs Antenna Length when gap is of 20 nm

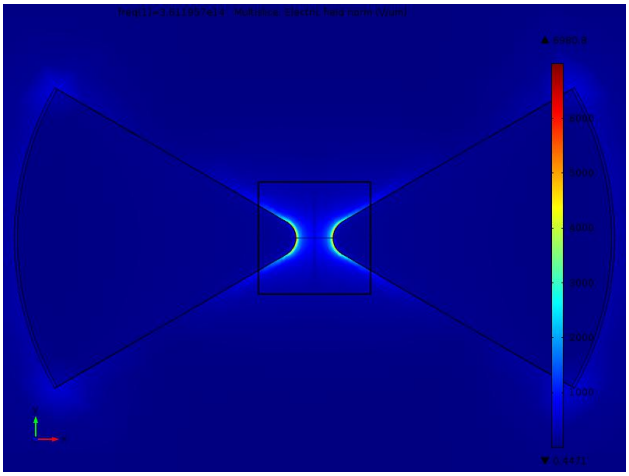

Figure 4.9: Electric field distribution around antenna when L = 140 nm and gap = 20 nm

It has been observed that the field enhancement is maximum in bow tie antenna. Also these results are in accordance with that of Cubukcu et al. There are some variation in values which can be attributed to the difference in software and material parameters.

4.3 Shuriken Shaped Nanoantenna

In this work a new design of nanoantenna is proposed for its application as solar energy harvester. Design of nanoantenna is in the shape of Shuriken. This antenna design is polarisation independent and is broadband in operation. Antenna is 1.43 μm long and 50 nm thick having the 25 nm as radius of curvature of edges. Antenna is placed over the silica substrate of refractive index n = 1.42 as shown in Fig 4.10.

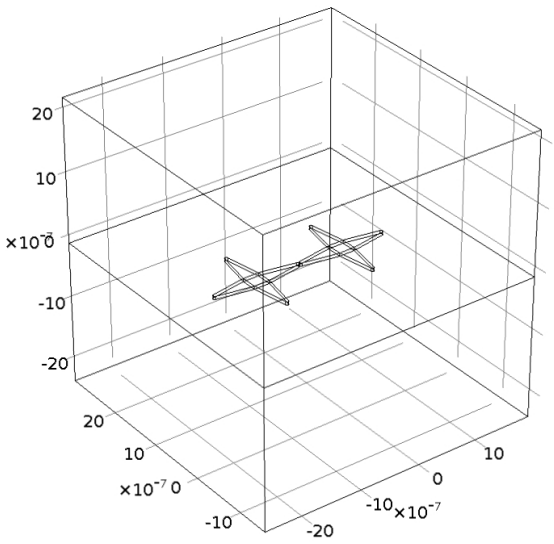

Figure 4.10: Coupled Shuriken Shaped Antenna placed over Silica substrate

Light of electric field intensity 1 V/m is incident vertically upon the antenna.The polarisation of incident light is in x direction. The material used for antenna are Copper and Gold.

Both far field and near field analysis of antenna is done.

4.3.1 Far field Analysis

In far field analysis half power beamwidth (HPBW), directivity and input impedance have been calculated along with the radiation pattern of the antenna. Radiation pattern is defined as graphical representation of the antenna properties as a function of space coordinates. It is determined in the far field region. Radiation pattern of Shuriken antenna is similar to that of dipole antenna. Coupled Shuriken antenna is used for the radiation pattern calculation. The radiation pattern and corresponding polar plot is shown in Fig 4.11.

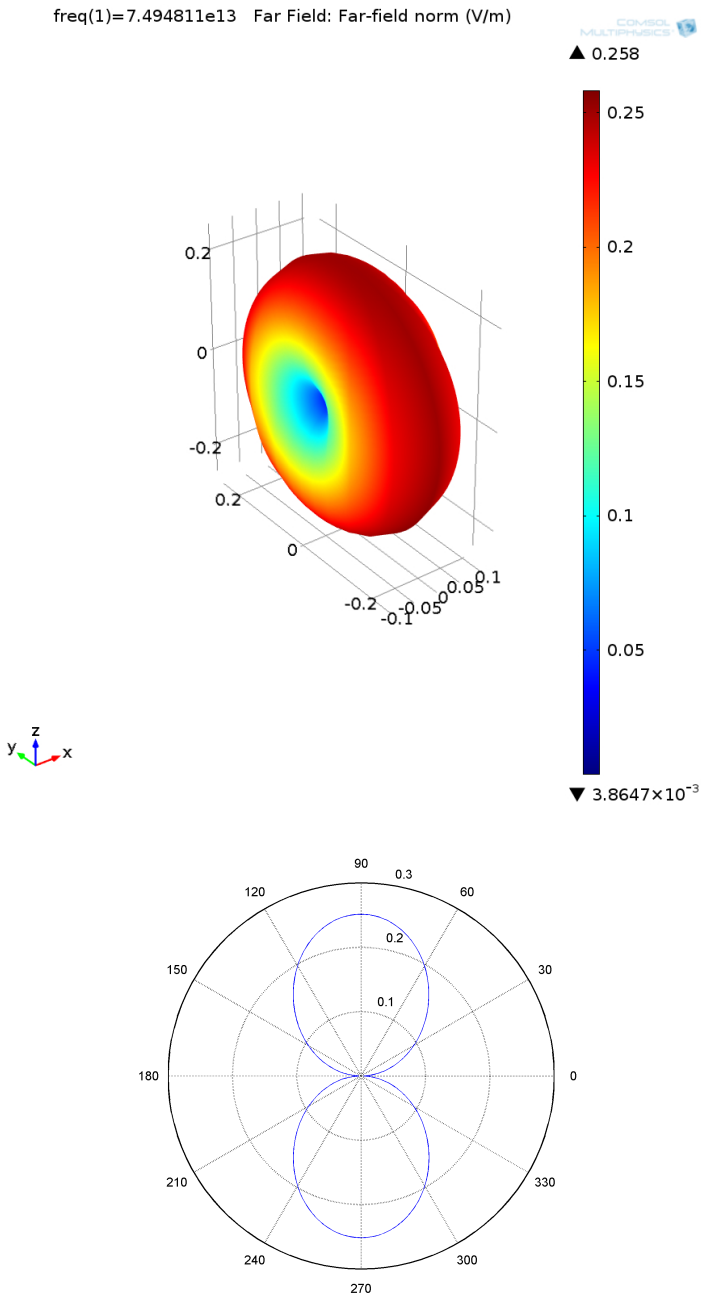

Figure 4.11: Radiation Pattern and Polar Plot of Coupled Shuriken Antenna

From the polar plot we can calculate the half power beamwidth(HPBW) of the antenna. IEEE defined half power beamwidth as angle between the two directions in which the radiation intensity is one-half value of the maximum

beam. HPBW as calculated from polar plot is 77.9^o.From the calculation of HPBW we can obtain directivity of the antenna. Directivity is defined as the ratio of the radiation intensity in a given direction from the antenna to the radiation intensity of isotropic antenna.

$$D = \frac{4\pi U}{P_{rad}} \tag{4.3}$$

Directivity can also be calculated using the HPBW. It is given as follows

$$D_o = \frac{4\pi}{\Omega_A} \simeq \frac{4\pi}{\Theta_{1r}\Theta_{2r}} \tag{4.4}$$

when HPBW is in radian.If HPBW is present in degree then above eqn can be written as

$$D_o \simeq \frac{4\pi(\frac{180}{\pi})^2}{\Theta_{1d}\Theta_{2d}} = \frac{41,253}{\Theta_{1d}\Theta_{2d}} \tag{4.5}$$

Here Θ_{1d}, Θ_{2d} are HPBW in one plane in degree and plane at 90^o to previous plane in degree. Directivity of coupled Shuriken antenna is $6.79 = 8.32$ dB.

Calculation of input impedance is done directly through antenna simulation. It is defined as the impedance presented by an antenna at its terminals or the ratio of the voltage to current at a pair of terminals. It is given as

$$Z_A = R_A + \iota X_A \tag{4.6}$$

For coupled Shuriken antenna its value is $88.9 + \iota\ 48.86\ \Omega$.

4.3.2 Near Field Analysis

In near field analysis of antennna scattering boundary condition has been used and electric field enhancement is calculated for single and coupled shuriken antennna. Optimization of coupled antenna system is done to enhance the performance and captured electric field.The performance of shuriken antenna depend upon its geometrical parametres such as thickness, gap between the antenna arms. The length and flare angle are 1.43 μm and 40^o respectively. These parametres are kept constant and calculation of electric field as a function of wavelength is done so as to obtain the resonant wavelength for the particular length and flare angle. Wavelength is varied from 1 μm to 10 μm.

When paramteric sweep in wavelength is given then it is observed that in single shuriken less electric field is obatined as compared to coupled shuriken antenna. Also the resonance peak in single shuriken antenna is occuring at

3.5 μm while in coupled it is shifted to 4.3 μm. It can be observed from the graph in Fig 4.12 and their electric field distribution is given as shown in Fig 4.13. In both the cases antenna is made up of copper.

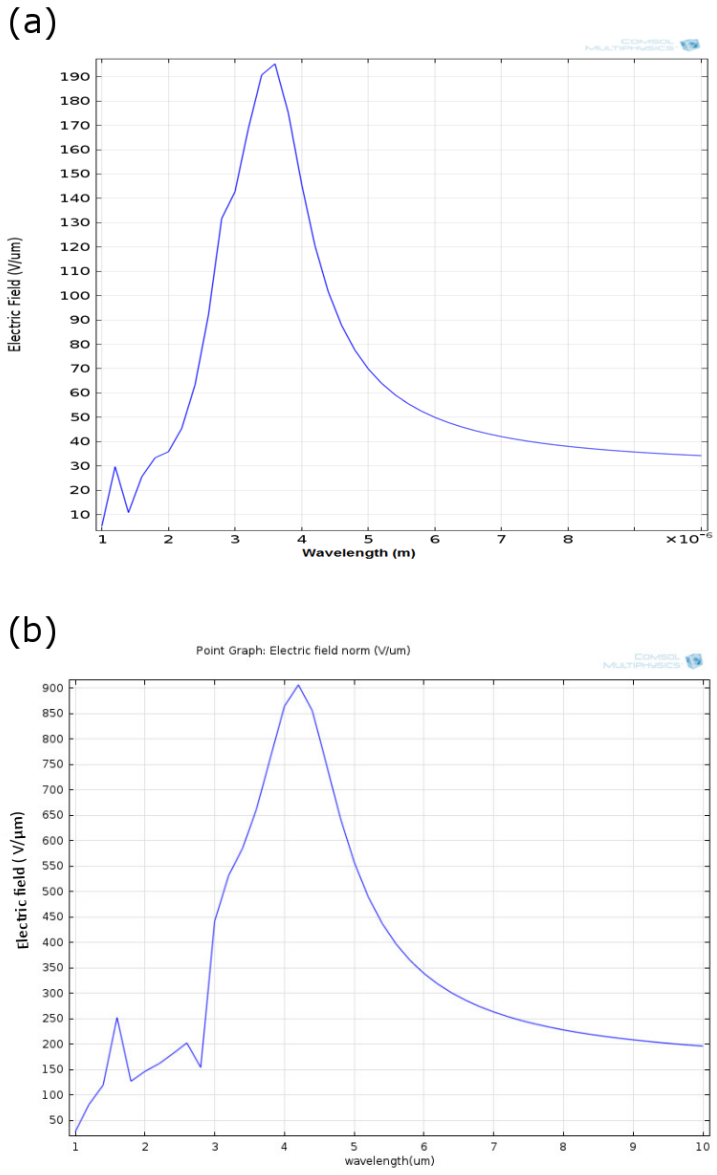

Figure 4.12: Electric Field Vs Wavelength (a). For Single Shuriken Antenna and (b). Coupled Shuriken Antenna

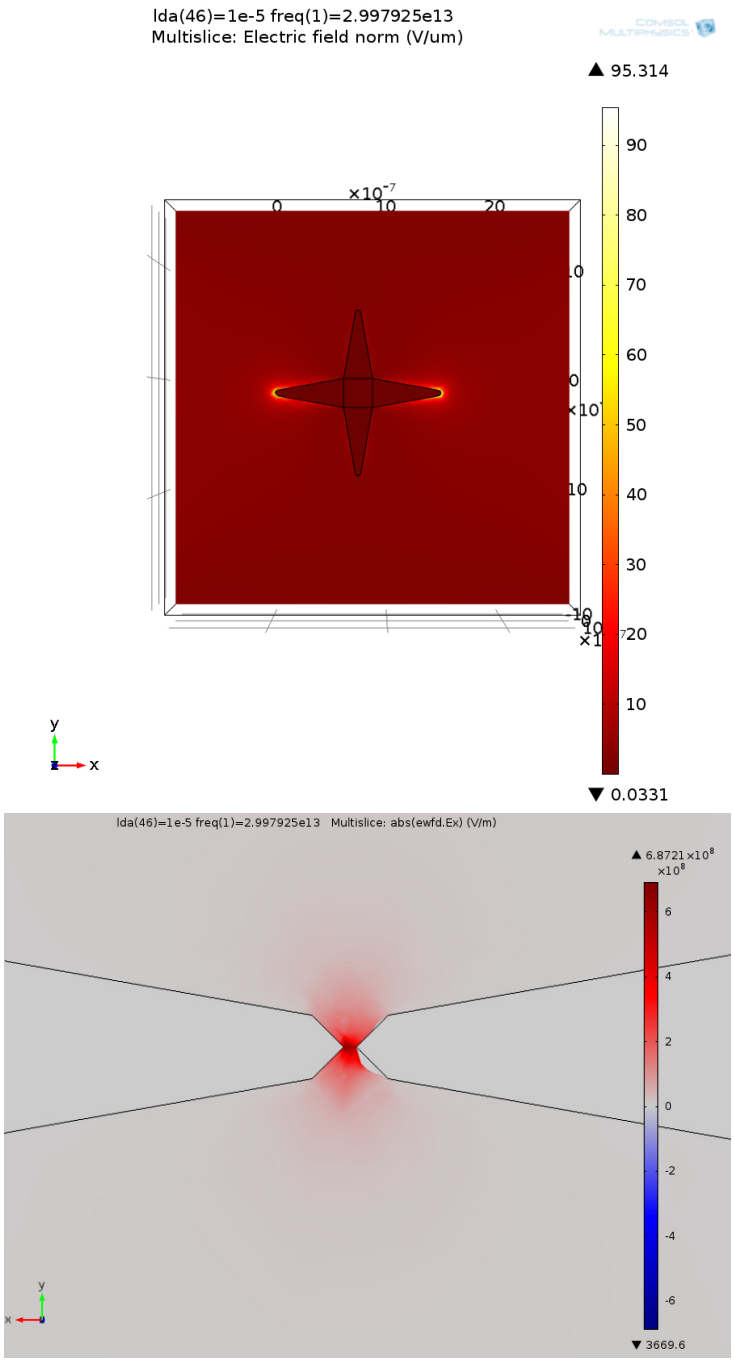

Figure 4.13: Electric Field Distribution in single and Coupled Shuriken antenna

From above observation it is clear that electric field enhancement is much more in coupled shuriken antenna because of localised surface plasmon res-

onance and lightning rod effect. So, it is best suited as energy harvester. But this enhancement is nearly same as that of bowtie antenna. For more enhancement one antenna element is made of gold and another of copper. Because of using dissimilar metals it is observed from graph in Fig 4.14 that more enhancement of electric field is occurring at the feed point.

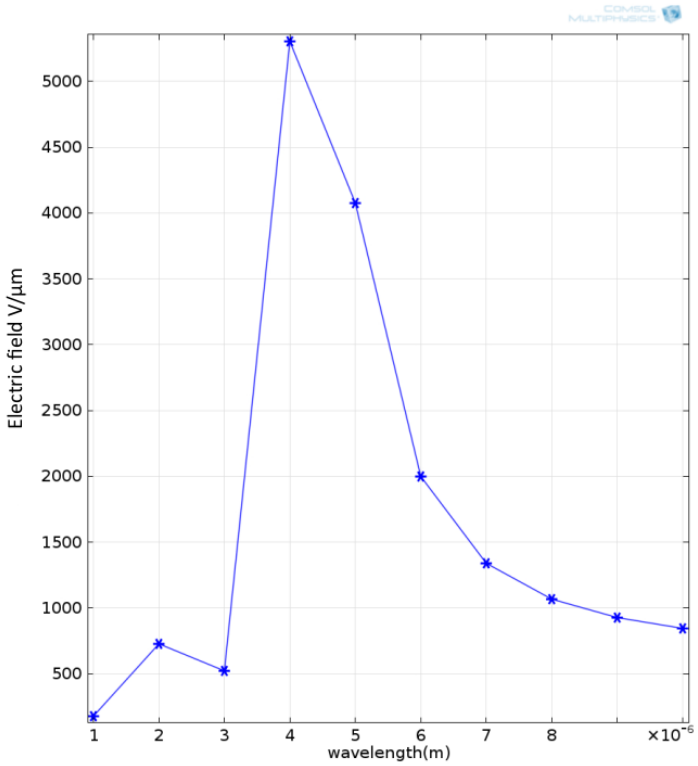

Figure 4.14: Electric Field Vs Wavelength when one shuriken is copper and another is of gold

The peak of resonance remain almost same as in the previous case which is $\simeq$ 4.3 μm. Electric field enhancement is almost 6 times in dissimilar metal antenna to that of similar metal Shuriken antenna.This nanoantenna is optimized for thickness of metal and gap between the antenna elements.

Effect of gap

Here gap is varied from 0 to 100 nm with step size of 5 nm and corresponding change in electric field is measured as shown oin Fig 4.15. When shuriken antenna made up of gold and copper are optimized for the gap between the

antenna element it is observed that electric field is maximum when gap is 5 nm and it gradually decreases after 5 nm. Beyond 60 nm effect of gap on electric field is negligible as change in electric field is almost constant. So, high intensity electric field is obtained when gap size is small. However to fabricate such a small size is a difficult task.

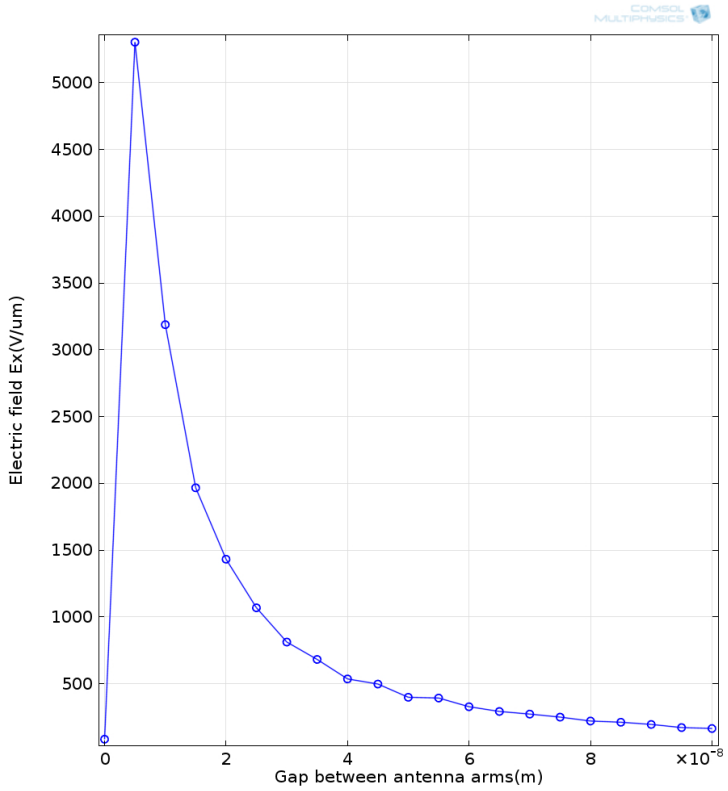

Figure 4.15: Electric field Vs Gap between antenna elements

Effect of Thickness

Effect of thickness on electric field is studied when thickness of the antenna is varied from 10 nm to 60 nm with step size of 5 nm. It is observed that maximum electric field is obtained at the thickness of 20 nm. Below 20 nm electric field decreases as losses are increased as quantum mechanical effect comes into play because of metal behaves as thin film. After 20 nm electric field decreases at 25 nm then increases and then finally decreases. These observations are shown in Fig 4.16. So, antenna should be of optimum thickness so that high electric field intensity is obtained and is easy to fabricate.

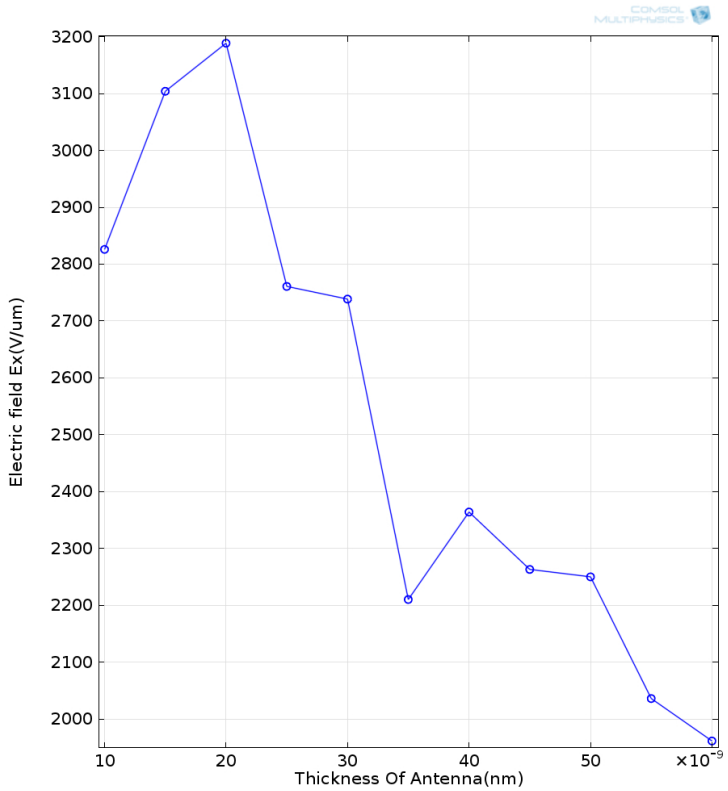

Figure 4.16: Electric Field is varied with the thickness of antenna for high electric field at the feed point

4.3.3 Optimized Nanoantenna

Nanoantenna is optimized in gap size and in thickness to resonate at 4 μm wavelength. So, gap size is taken as 5 nm and thickness is taken as 20 nm as electric field enchancement is very high at these dimensions in the feed point. Material parameters are determine by the Drude Model which is centered around 4 μm wavelength and light having 1 V/m electric field polarised in x direction is incident upon the antenna. The electric field enhancement in the optimised nanoantenna is given as follows in Fig 4.17;

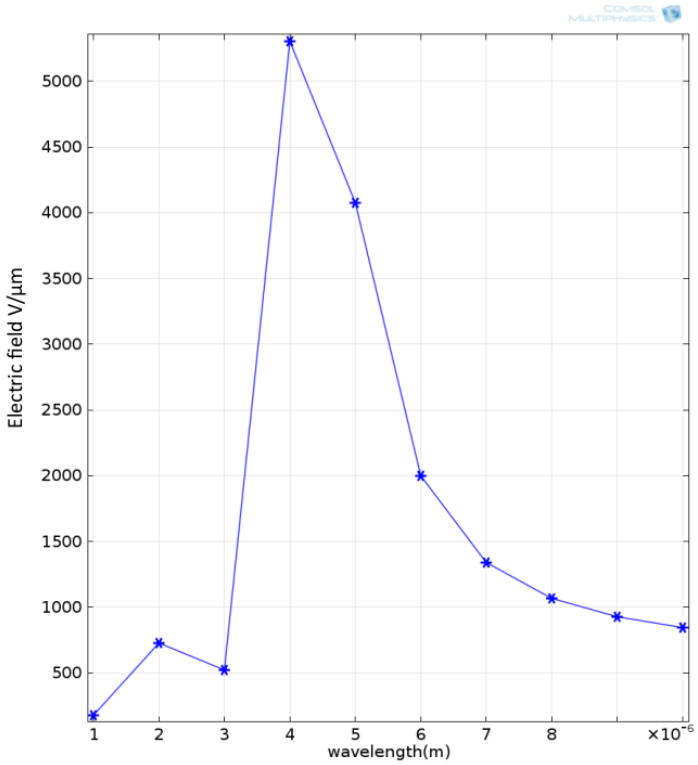

Figure 4.17: Electric Field Vs Wavelength when one shuriken is copper and another is of gold

Chapter 5

Analysis of Nanoantenna with MIM Diode

In this section detailed discussion on MIM diode is done along with the analysis of nanoantenna integrated with MIM diode.

5.1 Tunneling Effect

Tunneling is a quantum mechanical phenomenon in which electron pass through the potenial barrier without overcoming it. By the help of classical particle mechanics it cannot be explained because in classical mechanics under the influence of electric field repulsive force acts on the electrons which decreases the velocity till it comes to rest and then retreat backward with its reverse velocity while in wave mechanics there is finite probability of electron penetration beyond the point at which reflection took place in classical mechanics. This electron penetration is known as tunnel effect.

Following are the areas where tunneling plays an important role

- Current across the thin p-n junction in semiconductor,
- Current through the oxide layer IN MIM diode,
- Breakdown mechanism in dielectrics(Zener effect)

It is a majority carrier effect. Here the concept of quantum transition probability per unit time is used rather than transit time when the electron is tunneling through the potential barrier.Because of short tunneling time tunnel devices have very fast response time enabling them to work in high frequency region. They are mainly used in microwave and millimeter circuits as fast diodes.

5.1.1 Tunnel Diode

Leo Esaki in 1958, discovered a semiconductor diode which exhibits the negative resistance when diode is heavily doped. He used 10^3 impurity atoms for doping in 10^7 semiconductor atoms. Following I-V curve is obatined for tunnel diode when doping is very high[15].

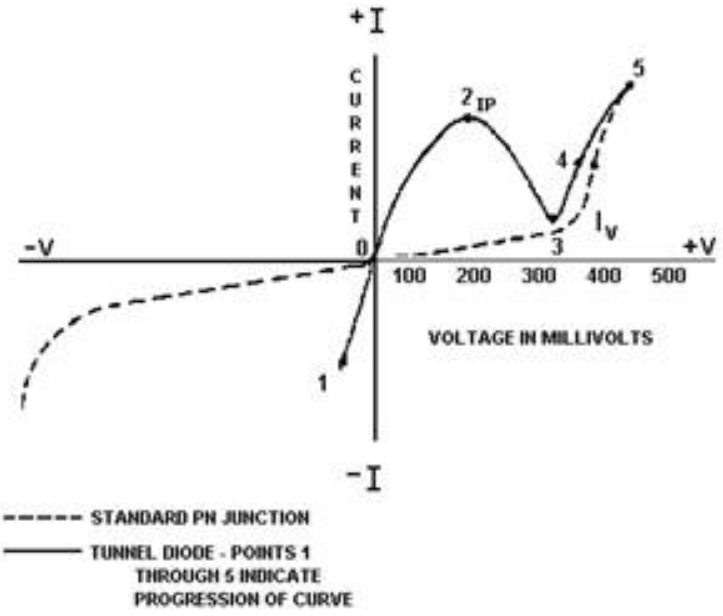

Figure 5.1: I-V characteristic curve of Tunnel Diode and P-N diode[15]

In semicondutor PN junction diode doping concentration is of order 1:10^8 atoms. Because of low doping, junction barrier is wide and electron can cross only if potential applied is more than that of junction potential. However in tunnel diode current increases till reaches the peak current ie I_p at point 2 as shown ih Fig 5.1. Beyond that, current starts decreasing with increase in voltage and reaches the lowest current value known as valley current I_v and is denoted as point 3. The region between I_p and I_v is called as negative resistance region and peak current occur due to the tunneling effect of electron. For tunneling to occur following conditions[24] are applied

- Doping should be very high so that barrier's width is very small.
- There should exists occupied energy states on side from where electrons has to tunnel
- There should exits free energy states where electron has to tunnel.
- Lastly, momentum of electron should be conserved.

5.2 Metal - Insulator - Metal Diode

In MIM diode a thin layer of oxide is placed in between the two layer of metals. So, that electron can tunnel through the insulator layer. Metal that are used can be simiiar or dissmiliar. These diode operate due to the tunneling effect. Tunneling occurs when the oxide layer thickness is in nanometer range. The I-V characteristic of diode is asymmetric if the metals that are used have large work function difference.These diodes are mainly used as THz detector. Some initially developed MIM diodes were point contact diode mainly Cat Whisker diode in which the Tungsten tip is pressed against the metallic base to form a tunnel junction. These diodes were mainly used for communication applications in GHz range.

5.2.1 Advantages of MIM Diode

Following are the advantages of MIM diode;

- These diodes have very fast response time[51] as tunneling takes very less time. So, they are very useful in THz range for IR and optical detection.
- Also, they have fast switching speed.
- In MIM diode due to the large barrier energy tunnenling current flows more than the dark current. Dark current flows in the device due to the thermally excited electrons at room temperature.
- Fabrication of thin film MIM diode is not so difficult and complex. They can be fabricated using ALD(Atomic Layer Deposition).

5.2.2 MIM Diode's Limitation

There are certain factor which affects the working of MIM diode in infrared and visible range. Parasitic capacitance is one factor which affects working of diode in high frquency range. Other factors include the mismatch between the antenna and diode resistance, diode characteristics such as linearity and symmetry, choice of metal to be use in diode.To work as rectifier in energy harvesting circuit diode should be non linear and asymmetric. Also, diode made of dissimilar metal rather than similar metal have higher conversion efficiency. Fabrication of diode is easy but they are realised only for laboratory purposes. Large scale fabrication is still a problem.

5.3 Basic Circuit of Antenna with MIM diode

Here in this subsection basic concept of antenna coupled with MIM diode is discussed. In the following circuit Fig 5.2 voltage source and R_A represents the antenna and antenna impedance whereas diode is represented by the R_D which is non linear in nature and in parallel capacitance is present which is represented as C[13].

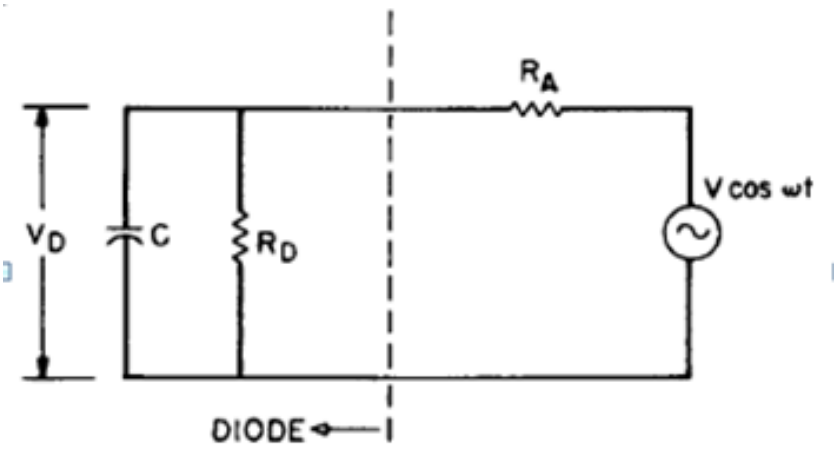

Figure 5.2: Basic circuit of Diode with antenna[13]

Power Calculation

According to *Sanchez et al.* maximum power delivered to the resistance R_D when there is no mismatch between the antenna and the diode resistance. For this, capacitance should have low value. Power obtained at the input of the diode is denoted by P_r and is delivered to the diode resistance given as

$$P_r = 2P_{in}\frac{1}{1+\sqrt{1+q}} \tag{5.1}$$

Here $q = \omega C R_a$, P_{in} is input power to the diode and P_r is the power delivered to the diode.P_r is maximum when $q << 1$. Matching in the Antenna-diode system is achieved when$P_r = P_in$ for $q << 1$.

Voltage and Current Rectification

Signals in THz range can be rectified by using MIM diode. This rectification property is due to the non linearity of diode.Voltage obtained in diode

contains harmonics having angular frequency ω along with the DC voltage. Expression of total voltage is as follows:

$$V_{tot} = V_d c + V_1(\omega) + V_2(2\omega) + V_3(3\omega) \tag{5.2}$$

whereas DC voltage varies due to the current at diode as function of bias voltage.

$$V_{rec} = \frac{-1I''(V_{bias})}{4I'(V_{bias})} v_{ac}^2 \tag{5.3}$$

v_{ac} is AC signal's amplitude around the diode. Rectified voltage for above circuit in terms of incident power can be given as

$$V_{rec} = \frac{4\beta_i P_{in} \frac{R_D^2}{R_A}}{1 + \frac{2R_D}{R_A} + \frac{(1+q^2)R_D^2}{R_A^2}} \tag{5.4}$$

Here $\beta_i = \frac{i_r}{P_r}$ which is responsivity due the current.So, rectified power can be given as;

$$P_{dc} = \frac{V_r^2}{R_D} \tag{5.5}$$

Cut-off frequency of diode is given as

$$f_c = \frac{1}{2\pi R_A C} \tag{5.6}$$

From above equation it is clear that C should be small as to achieve high cut off frequency. Also, the response time will be minimized.C can be reduced by minimizing the area of overlap as

$$C = \frac{\epsilon_o \epsilon_d A}{D} \tag{5.7}$$

where A is area of overlap and D is the thickness of oxide layer. Response time is given as e^{-t/CR_D}. Not only the value of Capacitance should be optimized so as to achieve high cut off frequency and fast response time and to obtain low diode impedance but oxide layer thickness should also be monitored to see the change in value of diode resistance.As low value of diode resistance is required for impedance matching with antenna. Electon Transmission probability is given by the wave equation

$$D = exp(-2d\frac{\sqrt{2m(V-E)}}{h/2\pi}) \tag{5.8}$$

where m is mass of electron,V is height of the potential barrier and d is thickness of oxide. So, for large tunneling probability thickness d of the barrier should be small.

5.4 Analysis of Antenna Integrated Diode

In this work a new design of nanoantenna is presented and idea is proposed in which the oxide layer is placed in between the overlapping arms of the metallic shuriken nanoantenna. The adjacent shurikens are of different metal.One is made up of Copper then another is of Gold. So, when thin oxide layer is placed in between the antenna arms it is sandwiched between the two different metals.This configuration is shown in the Fig as follows: This type of configuration is proposed because the field enhancement is more at the tip of antenna. Hence,diode is placed exactly at the tip.So, that enhanced field is directly coupled to the diode.

5.4.1 Simulation Results

In this subsection analysis of antenna is done when the arms of shurikens are overlapped with each other. Here elements of antenna are made up of two different metals Copper and Gold respectively. This done to make the asymmetric diode.When overlapping is done the electric field enhancement is seen in the gap between the antenna arms for the wavelength range of $2\mu m$ to 6 μm. The distribution of electric field is as shown in Fig 5.3

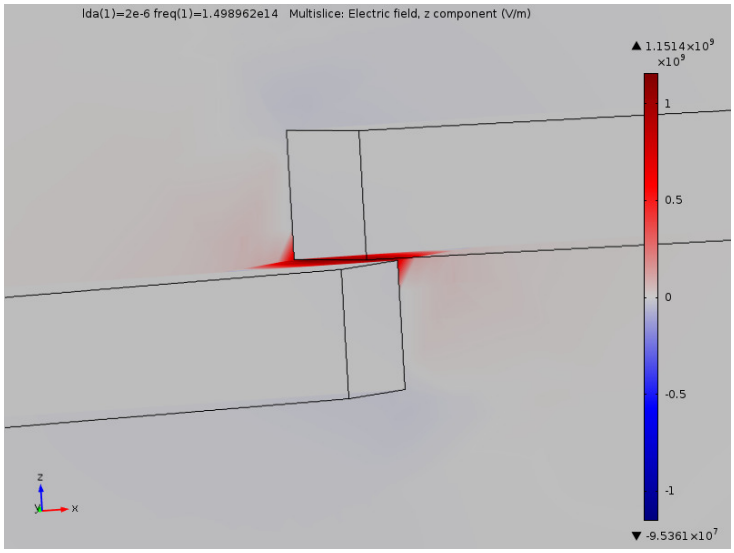

Figure 5.3: Electric field distribution when antenna arms are overlapped

Between the overlapped arms insulator is placed so as to make MIM diode. Here Copper oxide(CuO) is used as insulator and the resulting MIM

diode is Cu-CuO-Au. Due to the use of dissimilar metal the resulting diode will have asymmetric and non linear characteristics.

The oxide thickness is varied for different wavelengths. So, as to obtain the optimized thickness where high electric field is occurring. Oxide should be very thin i.e. below 100 A^o so that tunneling can easily takes place. In the graph(Fig 5.4) below the oxide thickness is varied as 2 nm, 3 nm,4 nm,5 nm, and 6nm for wavelength range of 2 μm-6 μm and it is observed that the maximum electric field is obtained for 3 nm and then 2 nm thickness and resonance peak is around 3.8 nm and 4.1 nm respectively. As operational wavelength is around 4 μm, so thickness should taken as 2.5 nm.

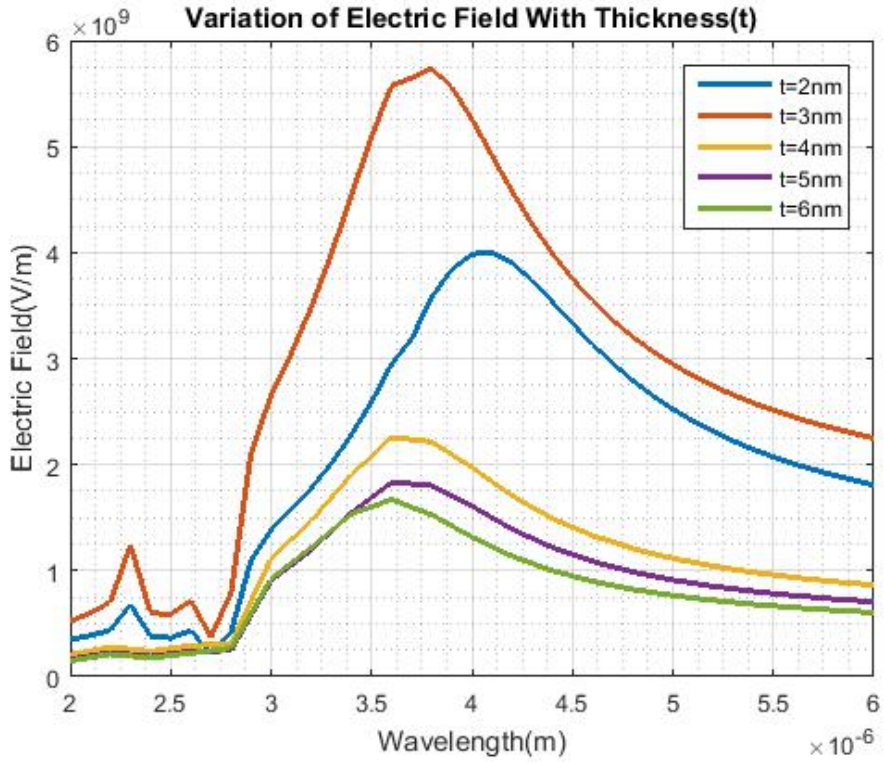

Figure 5.4: Variation of oxide thickness for different wavelengths.

Also, the overlapping area is varied for different wavelengths to obtained the optimized area. Overlapping area should be low. So,that the capacitance and resistance of diode should be low. This is done so as to obtain the high cut off frequency for diode. In the below graph(Fig 5.5) variation of overlapping area is shown when overlapped distance(d) is varied for different wavelengths. Maximum electric field is obtained when overlapped distance

is 20 nm and corresponding area is 5.75210^{-15} m^2 which is centered around $3.8\mu m$ wavelength.

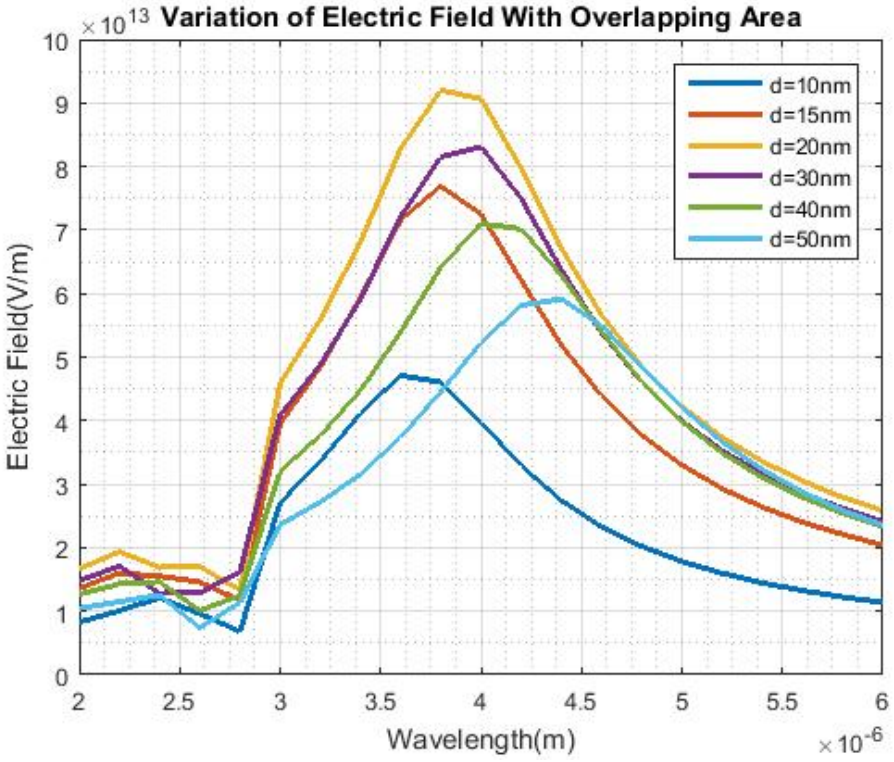

Figure 5.5: Variation of Overlapping area for different wavelengths where d is overlapped distance

As antenna is optimised for the overlapping area and diode thickness, voltage applied at the input of the MIM diode is measured for the insulator thickness of 2.5 nm when the overlappimng area is $5\times10^{-16}m^2$ as shown in Fig 5.6.

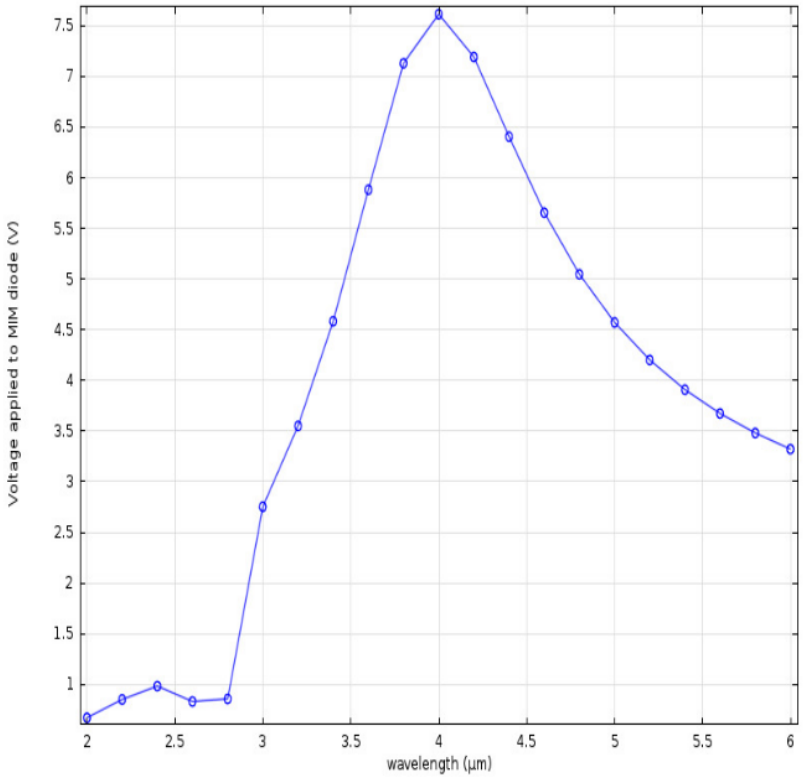

Figure 5.6: Voltage Applied at the diode surface

Design of antenna is such that it can work in x-polarised, y-polarised and both xy polarised incident light which makes the antenna polarisation independent. These coupled antenna can form array so as to utilise the benefit of design and to obtain the high electric field. In below Fig 5.7 electric field distribution in 2×2 array is shown when incident light is x polarised.

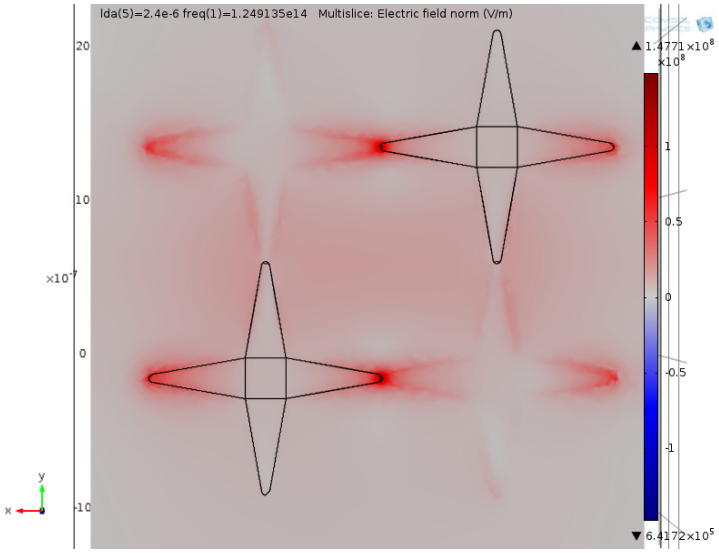

Figure 5.7: Electric field distribution in array of 2×2 when incident light is x-polarised

Charateristic of Diode

In the rectenna structure MIM diode plays an important role as it rectifies the incoming AC signal into DC signal.The I-V characteristics of diode helps in determining the responsivity(R), which gives the measure of the rectified DC. Zero bias resistance(R_D)and non linearity (N) can also be caluclated from I-V curve of diode where $R_D = \partial V/\partial I$, $N = \partial^2 I/\partial V^2$ and $R = \frac{\partial^2 I/\partial V^2}{\partial I/\partial V}$. The current density(J) can be calculated using the Simmons's expression given in eqn.2.1 and eqn 2.2.It is used for calculating the tunneling current across the insulator.To work as rectifier asymmetric and non-linear MIM diode is required.Asymmetric diode can obtained by using different types of metals on either side of the insulator.That's why MIM diode used here is made up of $Cu-CuO-Au$.The work functions of Au and Cu are ψ_{Au}= 5.47eV and ψ_{Cu} = 5.10eV respectively and electron affinity of the CuO is χ_{CuO} = 1.777 eV. The current density is plotted against the applied voltage using Simmon's formula as shown in Fig 5.8

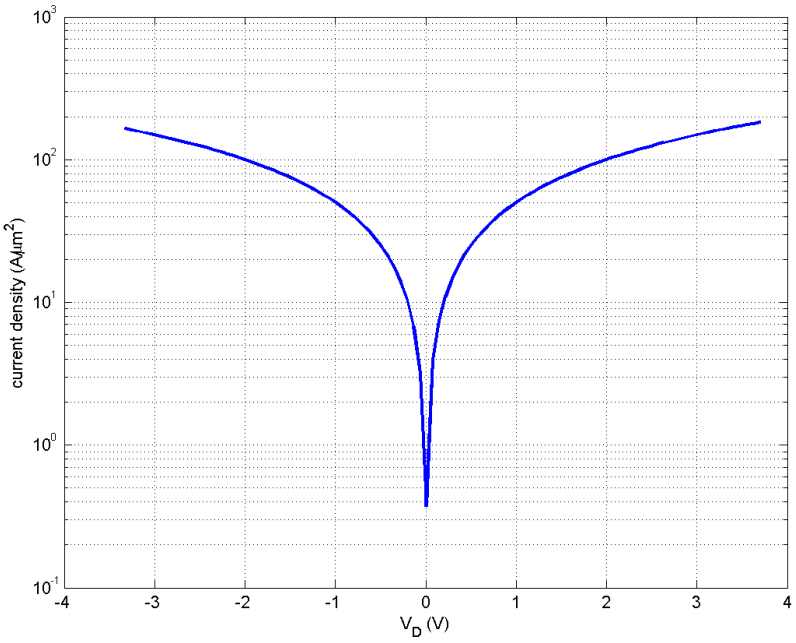

Figure 5.8: Currrent density versus applied voltage for $Cu-CuO-Au$ diode

Chapter 6

Conclusion and Future Work

6.1 Conclusion

In this research, far field and near field characteristics and application of nanoantenna as a energy harvester has been discussed along with the MIM diode. When nanoantenna is used in a circuit it enhances and localise the light in sub wavelength volumes. A novel design in shape of Shuriken has been proposed for nanoantenna which shows the promising results as compared to bowtie in terms of electric field enhancement and polarisation independence. This shuriken shaped antenna has been optimised for the gap size, thickness for a fixed length so as to resonate the antenna at 4 μm wavelength. Optimised antenna has length of 2.76 μm and gap of 5 nm exhibits electric field enhancement of 9 orders of magnitude. Because of such property nanoantenna can be used in many other applications such as near field microscopy, spectroscopy, as sensors other than the purpose of energy harvesting. In sub wavelength devices it can be used for guiding EM energy.

In this thesis, main application of antenna is to detect and rectify the IR wave for energy harvesting. This is done by coupling the antenna with MIM diode. Here, diode is made by placing the insulator (CuO) in between the overlapping arms of antenna made up of Copper and Gold. Again antenna along with MIM didoe has been optimised for thickness of insulator and area under the overlapping arms of antenna. It has been observed that high electric field enhancement is obtained at the insulator for thickness of 2.5 nm and $5\times10^{-}16$ m^2 area. Also, the voltage applied at the input of MIM diode has been calculated for different wavelength. Moreover, tunneling current density of diode has been calculated for a range of wavelength.

As mentioned above far field analysis has also been done and radiation pattern, Half power beamwidth(HPBW), directivity and input impedance is

calculated at 4 μm wavelength.

In summary, the result obtained in this work shows that the designed nanoantenna can be used in solar energy harvesting as it exhibits high electric field enhancement in the feed gap. Also, two or more antennas can be connected to make an array of nanoantennas. Here the designed antenna is polaristion independent so it can work in any polarisation like x, y and both xy in order to get high electric field at the output. For the efficient use of rectenna, antenna and MIM diode should be properly coupled so that there should be less impedance mismatch in the circuit. In the following section suggestions for the future work have been mentioned.

6.2 Future Work

There is still a long way to go to replace solar cells with rectenna. With all the research going on rectenna are still practically less efficient than solar cells. Research to make efficient rectenna is still in its infancy stage and there is a lot to achieve in this regard. So, it is difficult to cover all the aspects of this research in this thesis. Following are some ideas that is proposed so as to implement in future work.

- Optimize antenna on basis of materials and their permittivities.
- Optimize the antenna performance on the basis of mesh size.
- Compare the design of antennas for obtaining optimized and efficient antenna
- Fabricate the design proposed in the thesis and charcterize it.
- Use different numerical technique other than FEM for the computation.
- Obtain the I-V characteristics of MIM diode other than the current density and calculate the responsivity and efficiency.
- Design and characterise MIM diode having multiple layers of insulator i.e. MIIM and compare their performance with MIM diode.
- Apply other techniques such as transfer matrix method(TMM), the non-equilibrium Green's function(NEGF) and the quantum transmitting boundary method(QTBM).
- Finding an efficient techniques to interconnect the antenna within the arrays so as to obtain the enhanced electric field at the output.

References

[1] Bp statistical review of world energy, 2017.

[2] O Coddington, JL Lean, P Pilewskie, M Snow, and D Lindholm. A solar irradiance climate data record. *Bulletin of the American Meteorological Society*, 97(7):1265–1282, 2016.

[3] R Corkish, MA Green, and T Puzzer. Solar energy collection by antennas. *Solar Energy*, 73(6):395–401, 2002.

[4] William C Brown. The history of wireless power transmission. *Solar energy*, 56(1):3–21, 1996.

[5] B.W. C, G.R. H, H. Neil, and W.R. C. Microwave to dc converter, March 25 1969. US Patent 3,434,678.

[6] Robert Leo Bailey. A proposed new concept for a solar-energy converter. *Journal of Engineering for Power*, 94(2):73–77, 1972.

[7] Alvin M Marks. Femto diode and applications, January 19 1988. US Patent 4,720,642.

[8] Jörg P Kottmann, Olivier JF Martin, David R Smith, and Sheldon Schultz. Spectral response of plasmon resonant nanoparticles with a non-regular shape. *Optics Express*, 6(11):213–219, 2000.

[9] Dale K Kotter, Steven D Novack, WD Slafer, and PJ Pinhero. Theory and manufacturing processes of solar nanoantenna electromagnetic collectors. *Journal of Solar Energy Engineering*, 132(1):011014, 2010.

[10] Wenqi Zhu, Mohamad G Banaee, Dongxing Wang, Yizhuo Chu, and Kenneth B Crozier. Lithographically fabricated optical antennas with gaps well below 10 nm. *Small*, 7(13):1761–1766, 2011.

[11] Thorsten Feichtner, Oleg Selig, Markus Kiunke, and Bert Hecht. Evolutionary optimization of optical antennas. *Physical review letters*, 109(12):127701, 2012.

[12] Ahmed MA Sabaawi, Charalampos C Tsimenidis, and Bayan S Sharif. Planar bowtie nanoarray for thz energy detection. *IEEE Transactions on Terahertz Science and Technology*, 3(5):524–531, 2013.

[13] A Sanchez, CF Davis Jr, KC Liu, and A Javan. The mom tunneling diode: Theoretical estimate of its performance at microwave and infrared frequencies. *Journal of Applied Physics*, 49(10):5270–5277, 1978.

[14] Ertugrul Cubukcu, Nanfang Yu, Elizabeth J Smythe, Laurent Diehl, Kenneth B Crozier, and Federico Capasso. Plasmonic laser antennas and related devices. *IEEE Journal of Selected Topics in Quantum Electronics*, 14(6):1448–1461, 2008.

[15] Simon M Sze and Kwok K Ng. *Physics of semiconductor devices*. John wiley & sons, 2006.

[16] John Twidell and Tony Weir. *Renewable energy resources*. Routledge, 2015.

[17] World energy resources, 2016.

[18] Anna Mani. *Handbook of solar radiation data for India*. Allied Publishers, New Delhi (1080), 1980.

[19] P Bosshard, W Hermann, E Hung, R Hunt, and AJ Simon. An assessment of solar energy conversion technologies and research opportunities. *GCEP Energy Assessment Analysis*, 2006.

[20] Paolo Biagioni, Jer-Shing Huang, and Bert Hecht. Nanoantennas for visible and infrared radiation. *Reports on Progress in Physics*, 75(2):024402, 2012.

[21] Guang H Lin, Reyimjan Abdu, and John OM Bockris. Investigation of resonance light absorption and rectification by subnanostructures. *Journal of applied physics*, 80(1):565–568, 1996.

[22] James O McSpadden, Taewhan Yoo, and Kai Chang. Theoretical and experimental investigation of a rectenna element for microwave power transmission. *IEEE Transactions on Microwave Theory and Techniques*, 40(12):2359–2366, 1992.

[23] Young-Ho Suh and Kai Chang. A high-efficiency dual-frequency rectenna for 2.45-and 5.8-ghz wireless power transmission. *IEEE Transactions on Microwave Theory and Techniques*, 50(7):1784–1789, 2002.

[24] B Berland, L Simpson, G Nuebel, T Collins, and B Lanning. Optical rectenna for direct conversion of sunlight to electricity. In *National Center for Photovoltaics Program Review Meeting, NREL*, pages 323–324, 2001.

[25] Dale K Kotter, Steven D Novack, W Dennis Slafer, and Patrick Pinhero. Solar nantenna electromagnetic collectors. In *ASME 2008 2nd International Conference on Energy Sustainability collocated with the Heat Transfer, Fluids Engineering, and 3rd Energy Nanotechnology Conferences*, pages 409–415. American Society of Mechanical Engineers, 2008.

[26] Palash Bharadwaj, Bradley Deutsch, and Lukas Novotny. Optical antennas. *Advances in Optics and Photonics*, 1(3):438–483, 2009.

[27] Arvind Sundaramurthy, KB Crozier, GS Kino, DP Fromm, PJ Schuck, and WE Moerner. Field enhancement and gap-dependent resonance in a system of two opposing tip-to-tip au nanotriangles. *Physical Review B*, 72(16):165409, 2005.

[28] Holger Fischer and Olivier JF Martin. Engineering the optical response of plasmonic nanoantennas. *Optics express*, 16(12):9144–9154, 2008.

[29] MN Gadalla, M Abdel-Rahman, and Atif Shamim. Design, optimization and fabrication of a 28.3 thz nano-rectenna for infrared detection and rectification. *Scientific reports*, 4, 2014.

[30] Mena N Gadalla. *Nano Antenna Integrated Diode (Rectenna) For Infrared Energy Harvesting*. PhD thesis, 2013.

[31] Ragnar Holm. The electric tunnel effect across thin insulator films in contacts. *Journal of Applied Physics*, 22(5):569–574, 1951.

[32] JC Fisher and Ivar Giaever. Tunneling through thin insulating layers. *Journal of Applied Physics*, 32(2):172–177, 1961.

[33] John G Simmons. Generalized formula for the electric tunnel effect between similar electrodes separated by a thin insulating film. *Journal of applied physics*, 34(6):1793–1803, 1963.

[34] LO Hocker, DR Sokoloff, V Daneu, A Szoke, and A Javan. Frequency mixing in the infrared and far-infrared using a metal-to-metal point contact diode. *Applied Physics Letters*, 12(12):401–402, 1968.

[35] TK Gustafson, RV Schmidt, and JR Perucca. Optical detection in thin-film metal-oxide-metal diodes. *Applied Physics Letters*, 24(12):620–622, 1974.

[36] JG Small, GM Elchinger, Al Javan, Antonio Sanchez, FJ Bachner, and DL Smythe. ac electron tunneling at infrared frequencies: Thin-film m-o-m diode structure with broad-band characteristics. *Applied Physics Letters*, 24(6):275–279, 1974.

[37] C. Fumeaux, W. Herrmann, H. Rothuizen, P. De Natale, and F. K. Kneubühl. Mixing of 30 thz laser radiation with nanometer thin-film ni-nio-ni diodes and integrated bow-tie antennas. *Applied Physics B*, 63(2):135–140, 1996.

[38] Subramanian Krishnan, Shekhar Bhansali, Kenneth Buckle, and Elias Stefanakos. Fabrication and characterization of thin-film metal-insulator-metal diode for use in rectenna as infrared detector. In *MRS Proceedings*, volume 935, pages 0935–K03. Cambridge Univ Press, 2006.

[39] Prakash Periasamy, Jeremy D Bergeson, Philip A Parilla, David S Ginley, and Ryan P O'Hayre. Metal-insulator-metal point-contact diodes as a rectifier for rectenna. In *Photovoltaic Specialists Conference (PVSC), 2010 35th IEEE*, pages 002943–002945. IEEE, 2010.

[40] Philip CD Hobbs, Robert B Laibowitz, Frank R Libsch, Nancy C LaBianca, and Punit P Chiniwalla. Efficient waveguide-integrated tunnel junction detectors at 1.6 μm. *Optics express*, 15(25):16376–16389, 2007.

[41] Blake J Eliasson. Metal-insulator-metal diodes for solar energy conversion. *University of Colorado at Boulder, Ph. D. Thesis*, 2001.

[42] Matthew NO Sadiku and Shrikrishna V Kulkarni. *Principles of electromagnetics*. oxford university Press, 2015.

[43] Constantine A Balanis. *Advanced engineering electromagnetics*. John Wiley & Sons, 1999.

[44] C.A. Balanis. *ANTENNA THEORY: ANALYSIS AND DESIGN, 3RD ED (With CD)*. Wiley India Pvt. Limited, 2009.

[45] Andrea Alu and Nader Engheta. Theory, modeling and features of optical nanoantennas. *IEEE Transactions on Antennas and Propagation*, 61(4):1508–1517, 2013.

[46] Lukas Novotny. Effective wavelength scaling for optical antennas. *Physical Review Letters*, 98(26):266802, 2007.

[47] Stefan Alexander Maier. *Plasmonics: fundamentals and applications*. Springer Science & Business Media, 2007.

[48] Q-Han Park. Optical antennas and plasmonics. *Contemporary physics*, 50(2):407–423, 2009.

[49] MA Ordal, LL Long, RJ Bell, SE Bell, RR Bell, RW Alexander, and CA Ward. Optical properties of the metals al, co, cu, au, fe, pb, ni, pd, pt, ag, ti, and w in the infrared and far infrared. *Applied Optics*, 22(7):1099–1119, 1983.

[50] Mark A Ordal, Robert J Bell, Ralph W Alexander, Larry L Long, and Marvin R Querry. Optical properties of fourteen metals in the infrared and far infrared: Al, co, cu, au, fe, pb, mo, ni, pd, pt, ag, ti, v, and w. *Applied optics*, 24(24):4493–4499, 1985.

[51] Mordehai Heiblum, Shihyuan Wang, J Whinnery, and T Gustafson. Characteristics of integrated mom junctions at dc and at optical frequencies. *IEEE Journal of Quantum Electronics*, 14(3):159–169, 1978.